Global Biogeochemical Cycles

RESEARCH ARTICLE
10.1029/2019GB006265

Sinking of Gelatinous Zooplankton Biomass Increases Deep Carbon Transfer Efficiency Globally

Mario Lebrato[1,2], Markus Pahlow[3], Jessica R. Frost[4], Marie Küter[1], Pedro de Jesus Mendes[5], Juan-Carlos Molinero[3], and Andreas Oschlies[3]

[1]Geosciences Department, Christian-Albrechts-University Kiel (CAU), Kiel, Germany, [2]Bazaruto Center for Scientific Studies (BCSS), Benguerra Island, Inhambane Province, Mozambique, [3]GEOMAR Helmholtz Centre for Ocean Research Kiel, Kiel, Germany, [4]South Florida Water Management District, West Palm Beach, FL, USA, [5]Marine and Environmental Scientific and Technological Solutions (MAESTS), Bremen, Germany

Key Points:
- Gelatinous zooplankton link primary production to higher trophic levels and the deep ocean by serving as food and transferring jelly-C
- From global jelly-C production (0.038 Pg C year^{-1}) 59–72% reaches 500 m, 46–54% to 1,000 m, 43–48% to 2,000 m, 32–40% to 3,000 m, 25–33% to 4,500 m
- The jelly-C flux reaching the ocean interior is larger than anticipated for an important component of the global biological soft-tissue pump

Supporting Information:
- Supporting Information S1

Correspondence to:
M. Lebrato,
mario.lebrato@bcssmz.org

Citation:
Lebrato, M., Pahlow, M., Frost, J. R., Küter, M., de Jesus Mendes, P., Molinero, J.-C., & Oschlies, A. (2019). Sinking of gelatinous zooplankton biomass increases deep carbon transfer efficiency globally. *Global Biogeochemical Cycles*, *33*, 1764–1783. https://doi.org/10.1029/2019GB006265

Received 26 APR 2019
Accepted 11 DEC 2019
Accepted article online 17 DEC 2019
Published online 30 DEC 2019

Abstract Gelatinous zooplankton (Cnidaria, Ctenophora, and Urochordata, namely, Thaliacea) are ubiquitous members of plankton communities linking primary production to higher trophic levels and the deep ocean by serving as food and transferring "jelly-carbon" (jelly-C) upon bloom collapse. Global biomass within the upper 200 m reaches 0.038 Pg C, which, with a 2–12 months life span, serves as the lower limit for annual jelly-C production. Using over 90,000 data points from 1934 to 2011 from the Jellyfish Database Initiative as an indication of global biomass (JeDI: http://jedi.nceas.ucsb.edu, http://www.bco-dmo.org/dataset/526852), upper ocean jelly-C biomass and production estimates, organism vertical migration, jelly-C sinking rates, and water column temperature profiles from GLODAPv2, we quantitatively estimate jelly-C transfer efficiency based on Longhurst Provinces. From the upper 200 m production estimate of 0.038 Pg C year^{-1}, 59–72% reaches 500 m, 46–54% reaches 1,000 m, 43–48% reaches 2,000 m, 32–40% reaches 3,000 m, and 25–33% reaches 4,500 m. This translates into ~0.03, 0.02, 0.01, and 0.01 Pg C year^{-1}, transferred down to 500, 1,000, 2,000, and 4,500 m, respectively. Jelly-C fluxes and transfer efficiencies can occasionally exceed phytodetrital-based sediment trap estimates in localized open ocean and continental shelves areas under large gelatinous blooms or jelly-C mass deposition events, but this remains ephemeral and transient in nature. This transfer of fast and permanently exported carbon reaching the ocean interior via jelly-C constitutes an important component of the global biological soft-tissue pump, and should be addressed in ocean biogeochemical models, in particular, at the local and regional scale.

1. Introduction

Biological oceanic processes, primarily carbon production in the euphotic zone, sinking and remineralization, govern the global biological carbon soft-tissue pump (Buesseler et al., 2007). Sinking and laterally transported carbon-laden particles fuel benthic ecosystems at continental margins and in the deep sea (Koppelmann & Frost, 2008; Robinson et al., 2010). Marine zooplankton play a major role as ecosystem engineers in coastal and open ocean ecosystems because they serve as links between primary production, higher trophic levels, and deep-sea communities (Lebrato et al., 2012; Robinson et al., 2010; Robison et al., 2005). In particular, gelatinous zooplankton (Cnidaria, Ctenophora, and Chordata, namely, Thaliacea) are universal members of plankton communities that graze on phytoplankton and prey on other zooplankton and ichthyoplankton. They also can rapidly reproduce on a time scale of days and, under favorable environmental conditions, some species form dense blooms that extend for many square kilometers (Condon et al., 2013). These blooms have negative ecological and socioeconomic impacts by reducing commercially harvested fish species (Pauly et al., 2009), limiting carbon transfer to other trophic levels (Condon et al., 2011), enhancing microbial remineralization, and thereby driving oxygen concentrations down close to anoxic levels (Frost et al., 2012).

The global biomass of gelatinous zooplankton, herein collectively referred to as "jelly-carbon" (jelly-C), within the upper 200 m of the ocean amounts to 0.038 Pg C (Lucas et al., 2014). Calculations for mesozooplankton (200 μm to 2 cm) suggest about 0.20 Pg C (Moriarty & O'Brien, 2013). The short life span of most gelatinous zooplankton, from weeks up to 2 to 12 months (Ceh et al., 2015; Raskoff et al., 2003), suggests biomass-production rates above 0.038 Pg C year^{-1}, depending on the assumed mortality rates, which in

many cases are species-specific. This is much smaller than global primary production (50 Pg C $year^{-1}$) (Field et al., 1998), which translates into export estimates close to 6 Pg C $year^{-1}$ below 100 m (Moore et al., 2004; Siegel et al., 2014), depending on the method used. Globally, gelatinous zooplankton abundance and distribution patterns largely follow those of temperature and dissolved oxygen as well as primary production as the carbon source (Lucas et al., 2014). However, gelatinous zooplankton cope with a wide spectrum of environmental conditions, indicating the ability to adapt and occupy most available ecological niches in a water mass. In terms of Longhurst regions (biogeographical provinces that partition the pelagic environment; Longhurst, 1995, 1998), the highest densities of gelatinous zooplankton occur in coastal waters of the Humboldt Current, NE U.S. Shelf, Scotian and Newfoundland shelves, Benguela Current, East China and Yellow Seas, followed by polar regions of the East Bering and Okhotsk Seas, the Southern Ocean, enclosed bodies of water such as the Black Sea and the Mediterranean, and the west Pacific waters of the Japan seas and the Kuroshio Current (Brotz et al., 2012; Condon et al., 2012; Lucas et al., 2014). Large amounts of jelly-C biomass that are reported from coastal areas of open shelves and semienclosed seas of North America, Europe, and East Asia come from coastal stranding data (e.g., http://www.jellywatch.org/).

Large amounts of jelly-C are quickly transferred to and remineralized on the seabed in coastal areas, including estuaries, lagoons and subtidal/intertidal zones (reviewed in Lebrato et al., 2012), shelves and slopes (Billett et al., 2006; Lebrato & Jones, 2009; Sweetman & Chapman, 2011), the deep sea (Smith et al., 2014), and even entire continental margins such as in the Mediterranean Sea (Lebrato, Molinero, et al., 2013). Jelly-C transfer begins when gelatinous zooplankton die at a given "death depth" (exit depth), continues as biomass sinks through the water column, and terminates once biomass is remineralized during sinking or reaches the seabed, and then decays. Jelly-C per se represents a transfer of "already exported" particles (below the mixed later, euphotic or mesopelagic zone), originated in primary production since gelatinous zooplankton "repackage" and integrate this carbon in their bodies, and after death transfer it to the ocean's interior. While sinking through the water column, jelly-C is partially or totally remineralized as dissolved organic/inorganic carbon and nutrients (DOC, DIC, DON, DOP, DIN, and DIP; Chelsky et al., 2015; Sweetman et al., 2016; West et al., 2009), and any left overs further experience microbial decomposition or are scavenged by macrofauna and megafauna once on the seabed (Sweetman et al., 2014; Tinta et al., 2016). Despite the high lability of jelly-C (Ates, 2017; Sweetman et al., 2016), a remarkably large amount of biomass arrives at the seabed below 1,000 m. During sinking, jelly-C biochemical composition changes via shifts in C:N:P ratios as observed in experimental studies (Frost et al., 2012; Sempere et al., 2000; Titelman et al., 2006). Yet realistic jelly-C transfer estimates at the global scale remain in their infancy, preventing a quantitative assessment of the contribution to the biological carbon soft-tissue pump.

Ocean carbon export is typically estimated from the flux of sinking particles that are either caught in sediment traps (Asper, 1987) or quantified from videography (Jackson et al., 1997), and subsequently modeled using sinking rates (Martin et al., 1987). Biogeochemical models (e.g., Gehlen et al., 2006; Ilyina et al., 2013; Laufkötter et al., 2015) are normally parameterized using particulate organic matter data (e.g., 0.5–1,000 μm marine snow and fecal pellets) that were derived from laboratory experiments (Ploug et al., 2008) or from sediment trap data (Gehlen et al., 2006). These models do not include jelly-C (except larvaceans; Lombard & Kiørboe, 2010; Lombard et al., 2010) not only because this carbon transport mechanism is considered transient/episodic and not usually observed, and mass fluxes are too big to be collected by sediment traps (e.g., Siegel et al., 2014), but also because models aim to simplify the biotic compartments to facilitate calculations. Furthermore, jelly-C deposits tend not to build up at the seafloor over a long time, such as phytodetritus (Beaulieu, 2002), being consumed rapidly by demersal and benthic organisms (Sweetman et al., 2014) or decomposed by microbes (Tinta et al., 2016). The jelly-C sinking rate is governed by organism size, diameter, biovolume, geometry (Walsby & Xypolyta, 1977), density (Yamamoto et al., 2008), and drag coefficients (McDonnell & Buesseler, 2010). Recently, Lebrato, de Jesus Mendes, et al., 2013 determined the average sinking speed of jelly-C using Cnidaria, Ctenophora, and Thaliacea samples, which ranged from 800 to 1,500 m day^{-1} (salps: 800–1,200 m day^{-1}; scyphozoans: 1,000–1,100 m d^{-1}; ctenophores: 1,200–1,500 m day^{-1}; pyrosomes: 1,300 m day^{-1}). Jelly-C model simulations suggest that, regardless of taxa, higher latitudes are more efficient corridors to transfer jelly-C to the seabed owing to lower remineralization rates (Lebrato et al., 2011). In subtropical and temperate regions, significant decomposition takes place in the water column above 1,500 m depth, except in cases where jelly-C starts sinking below the thermocline. In shallow-water coastal regions, time is a limiting factor, which prevents remineralization while sinking

and results in the accumulation of decomposing jelly-C from a variety of taxa on the seabed. This suggests that gelatinous zooplankton transfer most biomass and carbon to the deep ocean, enhancing coastal carbon fluxes via DOC and DIC, fueling microbial and megafaunal/macrofaunal scavenging communities. However, the absence of satellite-derived jelly-C measurements (such as primary production; Behrenfeld & Falkowski, 1997) and the limited number of global zooplankton biomass data sets make it challenging to quantify global jelly-C production and transfer efficiency to the ocean's interior.

In this study, we use data from the recently published Jellyfish Database Initiative (JeDI: http://jedi.nceas.ucsb.edu; Condon et al., 2015), public data sets (http://www.bco-dmo.org/dataset/526852), and global biomass estimates of the upper ocean (Lucas et al., 2014) to model jelly-C transfer efficiency based on Longhurst biogeographical provinces. We estimate exit depths for individual gelatinous zooplankton phyla based on field vertical migration data. Combining these data with published sinking rates (Lebrato, de Jesus Mendes, et al., 2013) and vertical temperature profiles (compiled from GLODAPv2; Key et al., 2015) allow us to calculate remineralization curves and jelly-C transfer efficiency globally. Calculations use over 90,000 data points from 1934 to 2011 as a global representation, across the different phyla, and include separate values for each Longhurst Province. Using two different model functions, the aim of this study is to quantitatively address global biomass and jelly-C transfer efficiency, as well as the gelatinous zooplankton contribution to the sinking compartment of the biological soft-tissue pump. Our results suggest a high importance of including jelly-C transfer efficiency in the next generation of local and regional biogeochemical models, to consistently account for its potential role in global calculations.

2. Methods

2.1. Data Sources

In this study, gelatinous zooplankton and jelly-C refer to mesozooplankton (0.2 to 20 mm), macrozooplankton (20 mm to 20 cm), and megazooplankton (20 to 200 cm), following the Sieburth et al. (1978) scale. The majority of the observations of sinking jelly-C concern the macrozooplankton and megazooplankton. Gelatinous zooplankton biomass data originated from the Jellyfish Database Initiative (JeDI http://jedi.nceas.ucsb.edu; Condon et al., 2012), which is a global synthesis project that provides a public data set of nearly 500,000 data points, including quantitative, categorical, and presence-absence data for the last 400 years (see Lucas et al., 2014, for details; Figure 1). This project has a number of public databases in their open directories, including vertical migration data, which were accessed through http://www.bco-dmo.org/dataset/526852, and then arranged for modeling purposes in a CSV file (Figure 2; Appendix A). Readers can access data in the format used in this publication at the NOAA National Center for Environmental Information (NCEI) under Accession Number 0207402 in https://data.nodc.noaa.gov/cgi-bin/iso?id=gov.noaa.nodc:0207402. A limitation of the JeDI data set is that it does not cover the entire ocean (<50%), and it is also biased toward the Northern Hemisphere (43% vs. 23%) (Figure 1). The Southern Ocean, the West Pacific, the South East Pacific, and the South Atlantic are not well represented. This means that our jelly-C transfer efficiency total estimations from the upper-ocean gelatinous biomass (starting total production of 0.038 Pg C $year^{-1}$) are strongly conservative (see section 4). Although jelly-C exists below 200 m in the mesopelagic zone, for the purpose of this study we only used data from the upper 200 m because data from deeper depths are of poor quality and unreliable (Lucas et al., 2014). We do not use coastal stranding data in any of our calculations, all data are from the open ocean. Biomass data (in mg C m^{-3}) are calculated from abundance data following biometric equations (Lucas et al., 2011). These conversion factors are used because they were the most complete database at the time this study was developed and they were ready to be applied to our model. We acknowledge that there are more recent compilations of gelatinous zooplankton carbon estimations (Andersen et al., 2016) that could slightly reshape our modeled estimates. Biomass data are then classified as maximum and mean biomass by Longhurst Province, and finally further classified by phylum (Chordata, Cnidaria, and Ctenophora; Lucas et al., 2014; Figure 1; Appendix B).

2.2. Data Mining and Use in the Model

In order to estimate transfer efficiency, we calculate jelly-C microbial decay ratios between 1 and 0 to describe jelly-C remineralization profiles, which are based on vertical temperature profiles, species-specific sinking speeds, and empirical decay rates, for each Longhurst Province. For biomass data, mean and maximum values have been extracted from field data reported by Lucas et al. (2014) for the 43 Longhurst

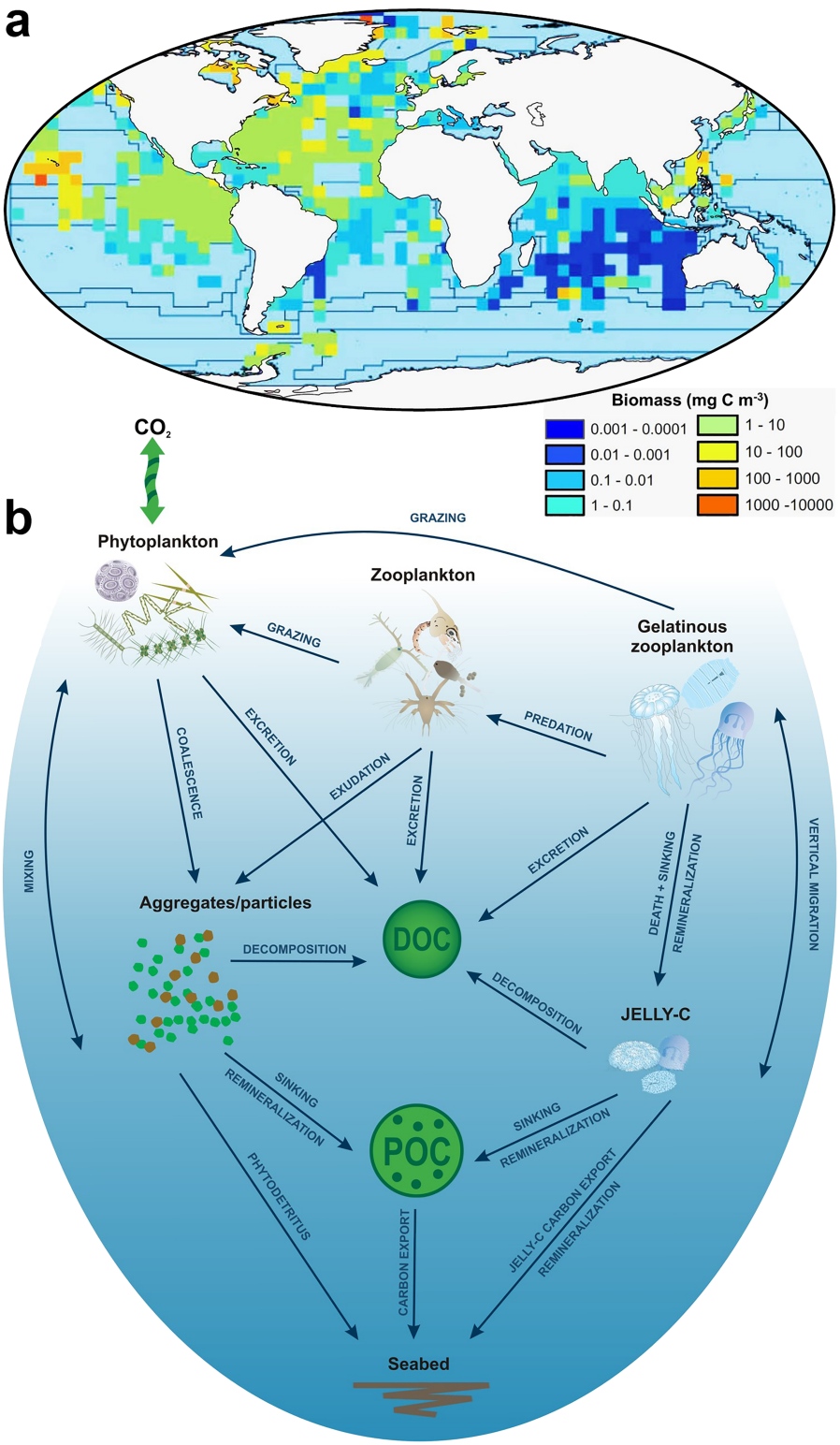

Figure 1. Global summary of gelatinous biomass and how jelly-C fits in the biological pump. (a) Upper ocean (200 m) depth-integrated global gelatinous zooplankton biomass on 5° grid cells displayed over the Longhurst Provinces modeled (light-blue/empty means no data available). Data are replotted as per Lucas et al. (2014) to model jelly-C export per Longhurst Province under John Wiley and Sons License Number 4575870755047. (b) A schematic representation of the biological pump and the biogeochemical processes that remove elements from the surface ocean by sinking biogenic particles including jelly-C. The diagram is adapted from a JGOFS U.S. cartoon to accommodate and describe jelly-C sinking and export. Symbols are courtesy of the Integration and Application Network (http://ian.umces.edu/symbols/).

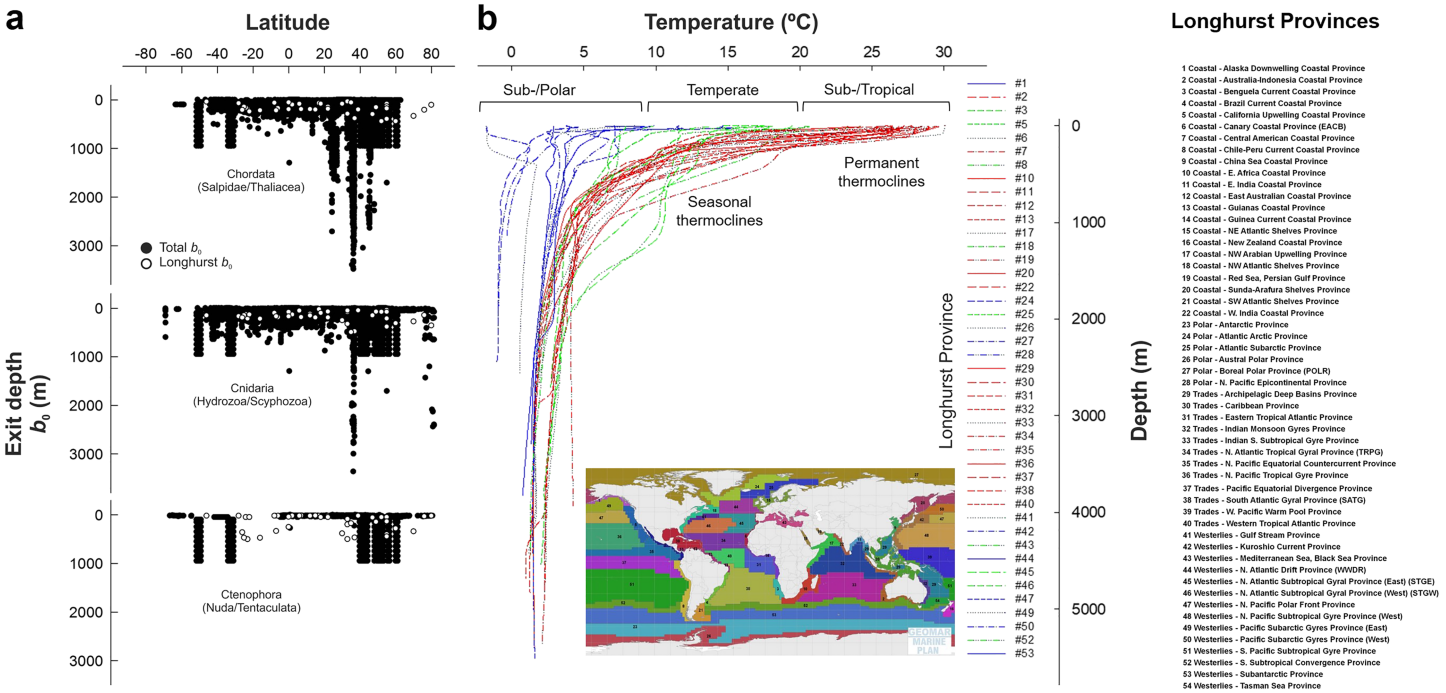

Figure 2. Latitudinal jelly-C exit depths and temperature profiles. (a) Detailed jelly-C exit depths (b0) vs. latitude for Chordata (Salpidae/Thaliacea), Cnidaria (Hydrozoa/Scyphozoa), and Ctenophora (Nuda/Tentaculata), including all available observations and the averaged b0 data used per Longhurst Province (details in Appendix C). (b) Representative vertical temperature profiles using GLODAPv2 data (Key et al., 2015) for each of the individual 43 Longhurst Provinces, used to model jelly-C export (details in Appendix B). Line colors correspond to latitude bands: Subpolar and Polar (blue), Temperate (green), and Subtropical and Tropical (red). Deepest temperature data coincide with the seabed depth, which allow calculating remineralization curves.

Provinces. Next, carbon transfer efficiency was calculated using combinations of exit depth (b0) and remineralization profiles (see below for details). The original data in Appendix B and Table S1, S2, S3, and S4 were extracted from Lucas et al. (2014) under John Wiley and Sons License Number 4575870755047.

Temperature data were extracted from the GLODAPv2 database (Key et al., 2015) (Figure 2; Appendix C) and classified according to latitude and longitude ranges of the 43 Longhurst Provinces and averaged into one representative vertical temperature profile per province (Appendices A and B). The representative temperature profiles are based on 50 to 100 temperature profiles per province, covering as much area as possible and spread out as evenly as possible using the same relative distance between profiles to avoid uneven weighting of areas within provinces with different densities of available temperature profiles. We acknowledge that a single Longhurst Province can have many different temperature profiles owing to the geographic range it occupies (Figure 2). Average seabed depth was also calculated from the GLODAPv2 database to feed the model with an end depth (b1) (Appendices A and B).

Based on the range of jelly-C sinking speeds (Lebrato, de Jesus Mendes, et al., 2013), we calculate mean global biomass export for nominal sinking speeds of 500, 1,000, and 1,500 m day^{-1}. Subsequently, assumed taxon-specific sinking speeds are used to obtain export estimates per phylum: Chordata (800 and 1,200 m day^{-1}), Cnidaria (900 and 1,100 m day^{-1}), and Ctenophora (500 and 1,300 m day^{-1}). Finally, a uniform sinking speed of 1,000 m day^{-1} is applied for all taxa to provide global biomass export estimates (Appendix B; Tables S1 and S2). We recognize that species-specific jelly-C sinking speeds could improve the calculations, but to the best of our knowledge, these estimates are the only ones available to date. We assume that carcasses sink in one piece, but we acknowledge potential fragmenting during sinking, which can change the sinking rate and also affect remineralization rate since smaller particles have larger surface area to volume ratio.

For exit depth ("death depth" = b0) (Figure 2) calculations, we assume that gelatinous zooplankton stay within their vertical migration depth range and do not undergo major predation. Since different species, classes, and phyla have different vertical migration ranges, and it is practically impossible to know at which depth they are dying, we assume that their deepest point of migration matches b0. The selection of a deep b0

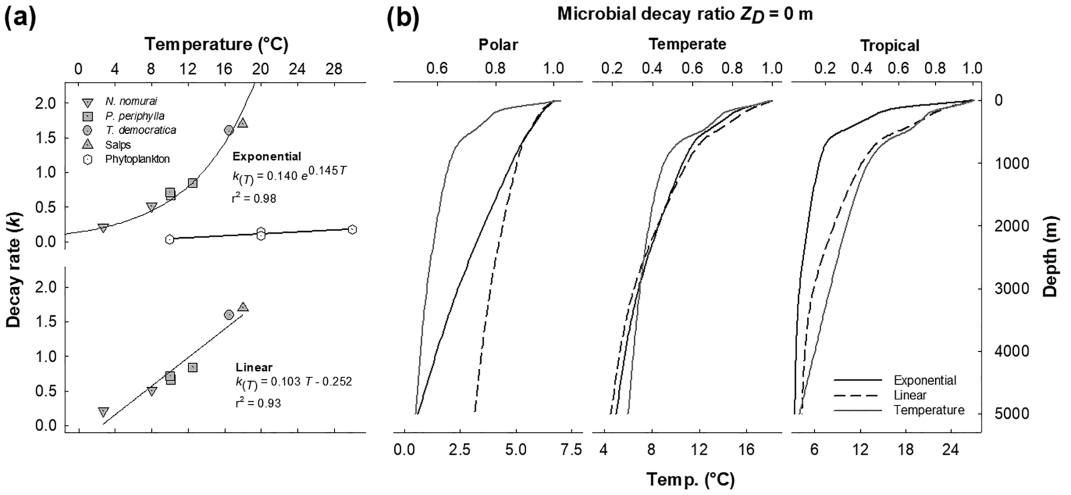

Figure 3. Temperature dependency equations and remineralization curves. (a) Decay rates (k) for exponential and linear temperature dependencies used to estimate jelly-C export curves in the 43 Longhurst Provinces. The linear equation is used to reduce the very high decay rates occurring at high temperatures when using the exponential function. For both curves $r^2 = 0.98$. (b) Both curves are compared using polar, temperate, and tropical temperature data to exemplify how they differ in terms of jelly-C transfer efficiency. Data for *Nemopilema nomurai* are from Iguchi et al. (2006), for *Perphylla perphylla* from Titelman et al. (2006), for *Thalia democratica* and for other Salps are from Sempere et al. (2000), and for phytoplankton from Sudo et al. (1978) and Fujii et al. (2002).

was made on the assumption that jelly-C does not stay floating in the surface, although in some cases it might, e.g., arriving to the shelves/neritic/beach areas. We think jelly-C, in general, starts sinking at depth because when organisms die, they are in a moribund state for a long time, slowly/passively sinking, until they eventually die off and sink faster. This has been observed in cruises/fieldwork around the world, and is often commented in cruise reports that find intact jelly-C at the seabed (e.g., Billett et al., 2006; Cacchione et al., 1978; Lebrato & Jones, 2009). Data are arranged geographically to match Longhurst Provinces and because variability exists in the number of b0 estimates per province (column "N° depths-counts" in Appendix B), depths (typically >50 depths per province) were averaged to provide a single "Longhurst death depth" per phylum and province (Figure 2, Appendices A and B). These estimates should be reliable for biomass data from b0 = 200–600 m, but we are apprehensive when it comes to biomass data deeper than b0 = 600 m due to poor or insufficient data (Lucas et al., 2014).

2.3. Model Development

The original model equation used to describe jelly-C transfer efficiency employs a decay rate (k, equation (1)) with exponential dependence on temperature (Lebrato et al., 2011). The model does not account for consumption influencing the decay rate, although it is known that jelly-C are further consumed by other organisms. The exponential relation is founded thermodynamically because many metabolic rates correlate exponentially with temperature, e.g., in aerobic heterotrophs the metabolic rate equals the respiration rate (Brown et al., 2004). Yet, when applying an exponential temperature equation (equation (2)), very quick biomass decay occurs at high temperatures based on a high bacterial remineralization coefficient (decay rate k) that may or may not be realistic. Experimental observations at the upper end of the temperature range used here (about 30 °C) are lacking. To account for this uncertainty, we approach this issue by introducing an alternative equation with k depending linearly on temperature (equation (3)) to reduce the effect of high temperatures on the biomass decay rates (Lebrato et al., 2011, and references therein, Figure 3, Appendices D and E). Results are presented for both equations to provide a range of jelly-C transfer efficiencies. Lastly, we compare both equations under different field (latitudinal) temperature conditions (Figure 2, Appendix D).

$$\frac{dM}{dt} = -k(T)\cdot M. \quad (1)$$

Jelly-C decay is calculated following first order kinetics with a decay constant (k) depending exponentially ($r^2 = 0.98$) or linearly on temperature (T), where T is represented by a gradient (exponential equation (2))

or a mean (linear equation (3)). While k may be expected to vary with organism size (Titelman et al., 2006), temperature accounts for 98% of the variability in k (equation (2); Figure 3a), even though the data encompass a wide range of sizes (0.1–1 kg wet weight). Solving equation (1) results in a jelly-C transfer efficiency (ratio) [M (z_R):M (z_D)] that relates initial biomass [M (z_D)], sinking from a given depth (z_D = death depth = b0) with temperature T (z_D), to a final biomass [M (z_R)], arriving at end depth (b1 = z_R) with temperature T (z_R), where z_R and T (z_{R-1}) are the end depth (seabed) and temperature in the water column, respectively. The depth z_D was obtained from the lower range of taxa vertical migration data (Figure 2). The data were independently collected and calculated per Longhurst Province and then applied in equations (2) and (3) below.

Jelly-C microbial decay ratios were estimated by solving (equation (1)) piecewise, dividing depth ranges into discrete depth intervals (Longhurst Province-specific; see Appendix B) using the two parameterizations for k below (Figure 3). In equations (2) and (3), C is Sinking Speed and $K_T(i)$ is the local temperature gradient between depths z_{i-1} and z_i. Underlying assumptions, calculations, and derivations of the solutions are available in Appendix E:

1. Exponential equation:

$$k(T) = 0.140\ \text{day}^{-1}\ e^{0.145°\text{C}^{-1}T(z)}. \tag{2}$$

Solution: $\frac{M(z_i)}{M(z_{i-1})} = e^{-\frac{0.140\text{day}^{-1}e^{0.145°\text{C}^{-1}T(z_{i-1})}}{0.145°\text{C}^{-1}K_T(i)C}\left(e^{0.145°\text{C}^{-1}K_T(i)\Delta z_i}-1\right)}, \Delta z_i = z_i - z_{i-1}$.

2. Linear equation:

$$k(T) = 0.064°\text{C}^{-1}\ \text{day}^{-1}\ T(z) + 0.02\ \text{day}^{-1}. \tag{3}$$

Solution: $\frac{M(z_i)}{M(z_{i-1})} = e^{-\frac{\Delta z_i}{C}\left[0.064°\text{C}^{-1}\text{day}^{-1}\left(T(z_{i-1})+\frac{K_T(i)}{2}\Delta z_i\right)+0.02\text{day}^{-1}\right]}$.

In both cases transfer efficiency is calculated as the product of the individual decay ratios of all depth intervals:

$$M(z_R) : M(z_D) = \prod_{i=1}^{n} M(z_i) : M(z_{i-1}), \tag{4}$$

where n is the number of depth intervals in each Longhurst Province and the local transfer efficiency M (z_i):M (z_{i-1}) is obtained with $k(T)$ from either equation (2), for exponential temperature dependence, or equation (3), for linear temperature dependence. An EXCEL spreadsheet is provided in the supplementary material (Appendix D) with the solution of equations (2)–(4), where users can type in their own data (Table 1; Appendix D).

2.4. Global Jelly-C Biomass Transfer Efficiency Estimations

In order to work out a global estimate of jelly-C arriving at the seabed, based on transfer efficiency, we grouped all Longhurst provinces data into three latitudinal bands, polar (66° to 90°, N and S), temperate (66° to 23°, N and S), and tropical (23° to 0°, N and S), using Appendix B to classify jelly-C biomass per Longhurst province and per latitudinal band. Then we averaged the representative vertical temperature profiles of all provinces in each latitude band to obtain one representative profile for each latitude band. Using the initial global standing stock of jelly biomass, M (z_R) = 0.038 Pg C from Lucas et al. (2014), we conservatively assume that organisms die after 1 year. Thus, our estimates remain an approximation given the short life span of many species, usually less than 1 year (Ceh et al., 2015; Raskoff et al., 2003). Regional biomass percentages are attributed to all Longhurst Provinces per latitudinal band, to determine how much biomass each latitudinal band contributes to the global standing stock of the database. The overall jelly-C biomass percentages are polar ~20%, temperate ~35%, and tropical ~45%. Using these percentages as initial biomass per latitudinal band plus the vertical temperature profiles, a constant sinking speed of C = 1,000 m day^{-1} and an exit depth of 100 m is used to determine the amount of jelly-C biomass transferred to each depth interval down to 6,000 m. Total jelly-C biomass transferred is reported below as the sum of the biomass per latitude band at each depth level. A single sinking speed and a single exit depth are chosen for the global estimation as an average of all the different scenarios encountered for all taxa, provinces, and sinking speeds

Table 1
Preview of the Excel Spreadsheet to Work Out Microbial Decay Ratios and Biomass for any Kind of Initial Conditions Using the Exponential and Linear Methods (Appendix S4)

Interval i (m)	Depths (m)		Temp. (°C)		K_T	M/M_0 interval	z_D-z_R (m)	M/M_0 final	Depth (m)	Biomass (mg C m^{-3})
EXPONENTIAL										
	b0	b1	tb0	tb1	Gradient	C = 1,300		1	0	20.000
0–100	0	100	27.00	24.00	−0.030	0.645	0–100	0.645	100	12.907
100–200	100	200	24.00	21.00	−0.030	0.753	0–200	0.486	200	9.722
200–500	200	500	21.00	18.00	−0.010	0.576	0–500	0.280	500	5.606
500-1,000	500	1,000	18.00	13.00	−0.010	0.594	0–1,000	0.167	1,000	3.330
1,000–3,000	1,000	3,000	13.00	8.00	−0.003	0.364	0–3,000	0.061	3,000	1.214
3,000–5,000	3,000	5,000	8.00	4.00	−0.002	0.593	0–5,000	0.036	5,000	0.721
LINEAR										
	b0	b1	tb0	tb1	Mean	C = 1,300		1	0	20.000
0–100	0	100	27.00	24.00	25.500	0.881	0–100	0.881	100	17.613
100–200	100	200	24.00	21.00	22.500	0.894	0–200	0.787	200	15.742
200–500	200	500	21.00	18.00	19.500	0.746	0–500	0.587	500	11.749
500–1,000	500	1,000	18.00	13.00	15.500	0.678	0–1,000	0.398	1,000	7.961
1,000–3,000	1,000	3,000	13.00	8.00	10.500	0.345	0–3,000	0.137	3,000	2.745
3,000–5,000	3,000	5,000	8.00	4.00	6.000	0.537	0–5,000	0.074	5,000	1.475

Note. Depth, temperature, and sinking speed parameters to change depending on working needs (EXCEL file in Appendix S4). z_0 = Exit depth ("death depth"); T (z) = Temperature at depth z; K_T = Temperature gradient between individual depths; M/M_0 = Microbial decay ratio between two adjacent depths; C = Sinking rate (m day^{-1}); z_D-z_R = Accumulated depth interval; M/M_0 final = Multiply individual microbial decay ratios to integrate the previous remineralization intervals; Biomass = Use initial biomass as a function of M/M_0 and then multiply by the previous number to integrate the remineralization intervals.

3. Results

Most b0 data (over 95%) in the database are within the upper 1,000 m, over 80% within 600 m (Figure 2; Appendices A and B). Only at a few latitudes we find b0 deeper than 600 m, which we exclude from further analysis. In most Longhurst Provinces and phyla, b0 lies within the upper 200 m, with some exceptions near 500 m. The averaged temperature profiles reflect our division of the Longhurst Provinces into tropical, temperate, and polar latitude bands, with permanent, seasonal, and absent thermoclines, respectively (Figure 2; Appendix C). We consider all export to below the permanent thermoclines as permanently exported to the ocean interior. Except for polar regions, temperature profiles converge between 3°C and 8°C below 1,000 m, with a semiconstant temperature below. The use of exponential and linear equations of decay rate (k) vs. temperature results in different microbial decay ratios for polar and tropical but not for temperate latitudes.

Jelly-C transfer efficiency depends on initial biomass, initial depth, end depth, sinking speed, and the temperature dependence (exponential is preferred for mechanistic reasons) (Figure 4). The microbial decay ratio is very sensitive to the exit depth (b0 = 100, 500, or 1,000 m) and end depth, which largely determine how much jelly-C arrives at the seabed (transfer efficiency >20% in most cases) (Figure 4). Varying sinking speed at b0 between 500 and 1,500 m day^{-1} changes how much jelly-C is transferred from b0 to the seabed by 5% to 15%. The equation for the temperature dependency (exponential or linear) also affects the estimated jelly-C transfer efficiency, with changes between 5% and 15% for the same b0 and sinking speed (Figure 4). The largest remineralization within the water column occurs in tropical regions, followed by temperate and polar regions. In most polar regions, remineralization is minimal, with over 70% of jelly-C arriving at the seabed. The same patterns are observed when using phylum-based ratios, but differences exist among the phyla (Figure 5). Each phylum has its own b0 per Longhurst province, which is reflected in the remineralization curves (Figure 5). Most remineralization occurs above 1,000 m, irrespective of b0 and sinking speed, with low remineralization rates below.

Jelly-C (mg C m^{-3}) maxima per Longhurst Province are used to determine biomass transfer efficiency under a mass deposition event scenario, as when a blooming population of gelatinous zooplankton completely collapses (Figure 6). Simulations for each phylum with multiple sinking speeds show that large quantities of jelly-C can reach the seabed at anytime and anywhere, irrespective of latitude, depth, sinking speed, b0,

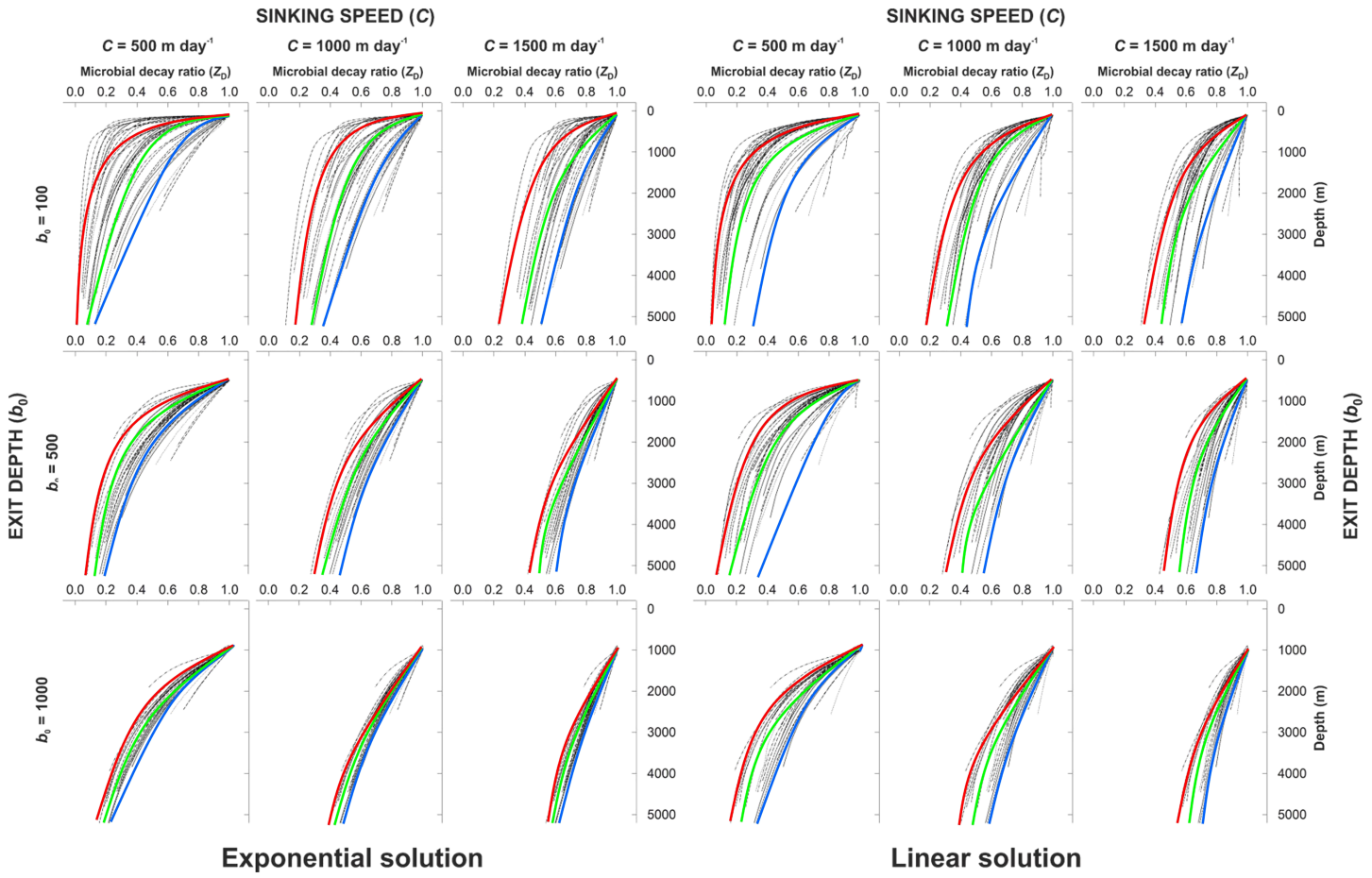

Figure 4. Global jelly-C transfer efficiencies using exponential and linear temperature dependencies. The microbial decay ratio (z_D) is calculated for individual averaged temperature profiles obtained from GLODAPv2 (Key et al., 2015) using data from 43 individual Longhurst Provinces. The plots use a matrix of three sinking speeds (500, 1,000, and 1,500 m s^{-1}) and three exit depths (b0) (100, 500, 1,000 m) to represent most field scenarios. The colored lines indicate the averaged polar (blue), temperate (green), and tropical (red) profiles.

or temperature dependence, assuming no major consumption from pelagic organisms (the percentage consumed is not known). During large bloom events in specific areas, with peaks from 1–5 g C m^{-3} to greater than 10 g C m^{-3} (averages per Longhurst province range from 5 to 15 mg C m^{-3}), most jelly-C biomass reaches the seabed (50% to 90%, Appendix C). Surprisingly, water depth (b1) is not a limiting factor and model predictions show that large quantities of jelly-C (>50% of original biomass) can arrive at 5,000 m and even deeper. In general, Cnidaria and Urochordata have the highest transfer efficiency, followed by Ctenophores. In some specific areas, Cnidaria have biomass maxima of ~20 g C m^{-3}, of which over 9 g C m^{-3} arrives at 5,000 m, but the average per Longhurst Province remains below 20 mg C m^{-3}. Given that in many oceanic areas, the seafloor is much shallower than 5,000 m, especially at continental margins, a large fraction of the jelly-C is transferred to the seafloor under a mass deposition event sinking at high speed (Figure 6). The only exceptions are shallow shelves where jelly-C could be remineralized or resuspended and mixed upward later during winter mixing.

Estimates of mean and maximum jelly-C biomass reaching the seabed differ between Longhurst Provinces, in some cases by several orders of magnitude (Figure 7; Tables S1 and S3). Variations between phyla range from near zero in some provinces to one or two orders of magnitude in others, reflecting the extreme complexity of jelly-C spatial distribution and transfer efficiencies (Figure 8; Tables S2 and S4). The total transfer of global jelly-C biomass across tropical, temperate, and polar regions also varies with the water depth being used as a target depth and temperature dependence used. Assuming a (conservative) global ocean total estimate of 0.038 Pg C $year^{-1}$ (Lucas et al., 2014), jelly-C biomass transfer summed over all areas is 0.022–0.027 Pg C $year^{-1}$ at 500 m, 0.016–0.018 Pg C $year^{-1}$ at 1,000 m, and 0.009–0.012 Pg C $year^{-1}$ at 4,500 m

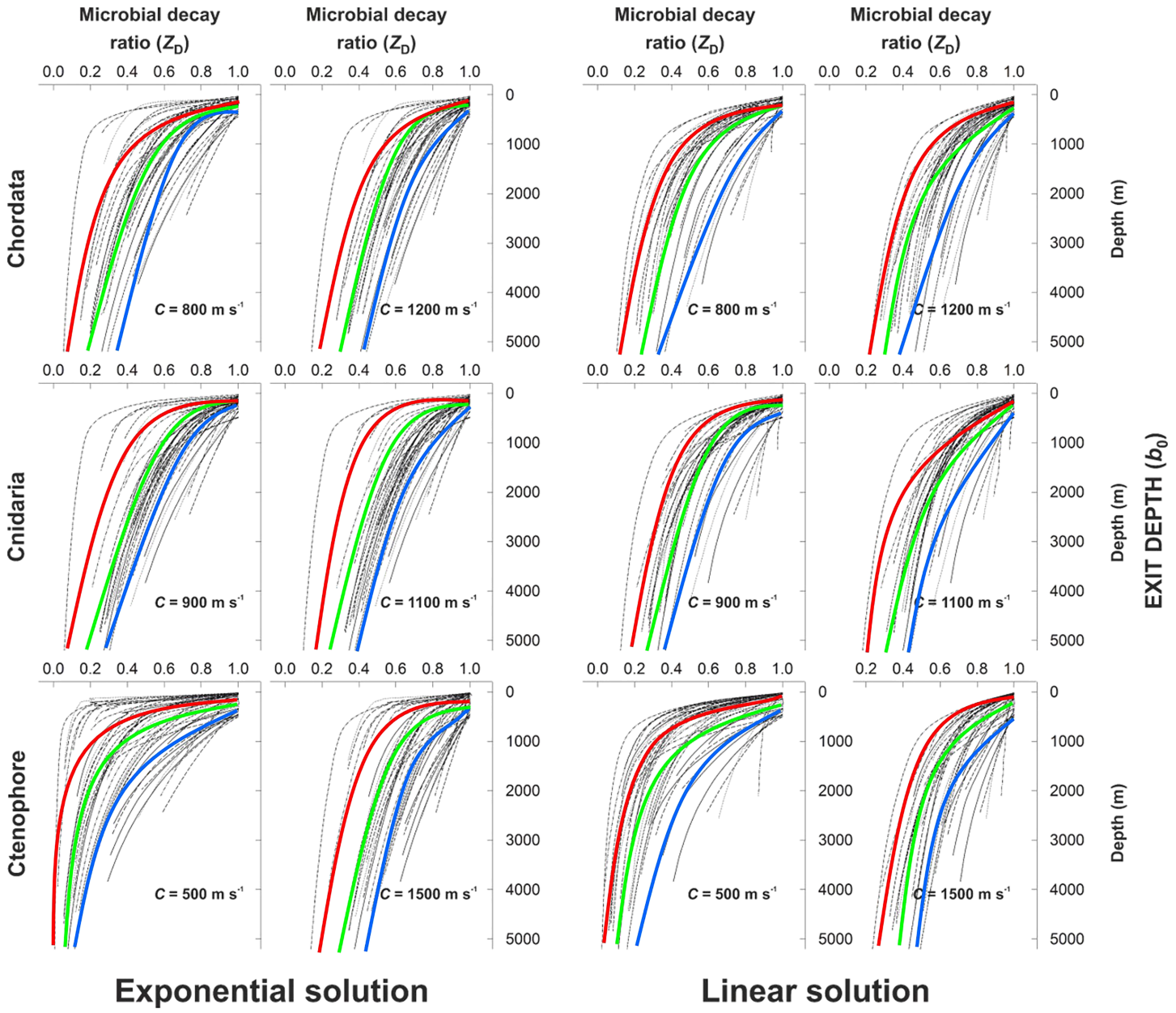

Figure 5. Phylum-province specific jelly-C transfer efficiencies using exponential and linear temperature dependencies. The microbial decay ratio (z_D) is d for individual averaged temperature profiles obtained from GLODAPv2 (Key et al., 2015) using data from 43 Longhurst Provinces. The plots use a matrix of two sinking speeds (phylum-specific using published data) and the 43 Longhurst Province specific exit depths (b0) (see Figure 2) to represent as accurately the field scenarios. The colored lines indicate the averaged polar (red), temperate (green), and tropical (blue) profiles.

(Figure 9). Jelly-C transfer to deeper than 4,500 m and export of biomass to the seafloor occur regularly (<0.010 Pg C).

4. Discussion

4.1. Transfer Efficiency of Sinking Jelly-C

Organic carbon originating in primary production follows three major pathways when sinking in the water column: (i) transfer to higher trophic levels during zooplankton grazing/filtering/consumption, (ii) export to depth via zooplankton fecal pellets/housings/biomass, and (iii) export through sinking of intact phytoplankton cells (phytodetritus) and marine snow/aggregates (Legendre, 1990; Peinert et al., 1989; Pilskaln & Honjo,

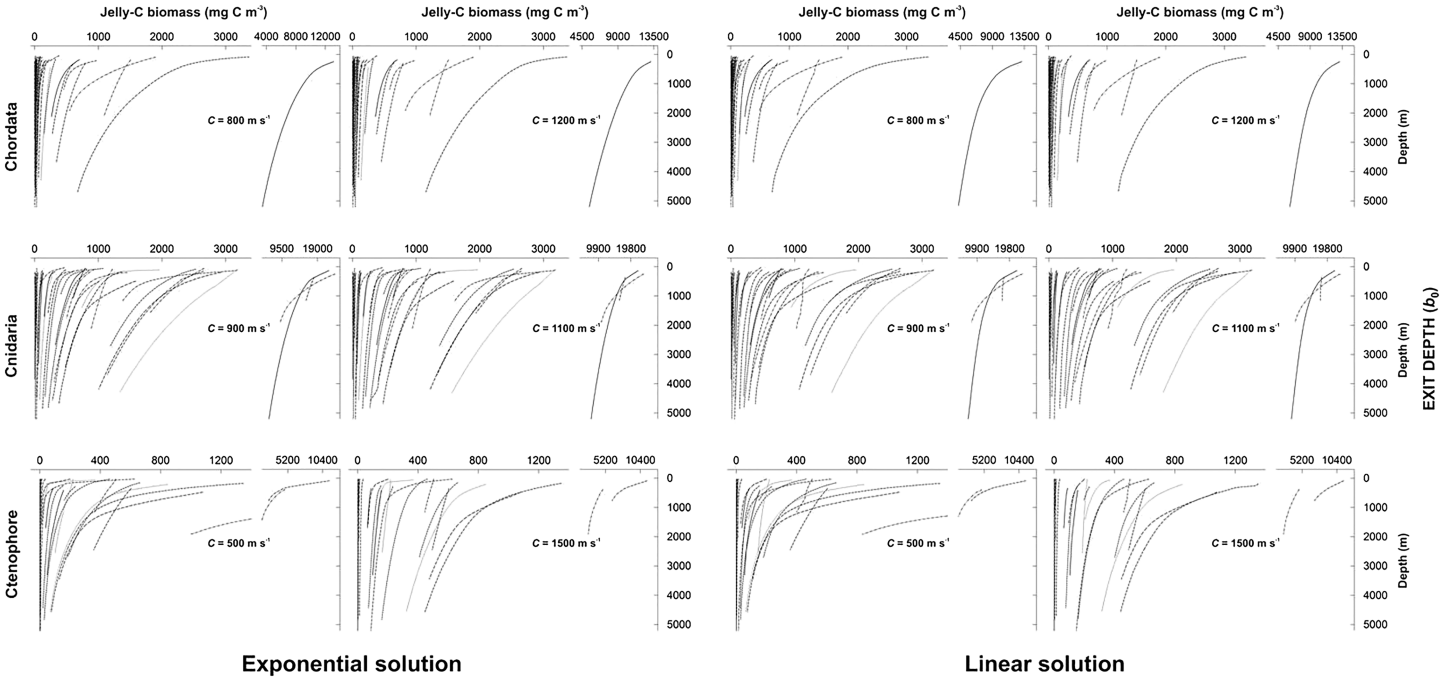

Figure 6. Phylum-province specific jelly-C biomass remineralization curves to show potential for seabed mass deposition. A summary of mean and maximum export values can be checked in Tables S1, S2, S3, and S4 and in Appendix B. Curves are calculated using exponential and linear temperature dependencies for individual average temperature profiles obtained from GLODAPv2 (Key et al., 2015) using data from the 43 Longhurst Provinces. The plots use a matrix of two sinking speeds (phylum-specific using published data) and the 43 Longhurst Province specific exit depths (b0) (see Figure 2) to represent as accurately the field scenarios. For ID of the Longhurst Provinces vertical profiles see Figure 2b.

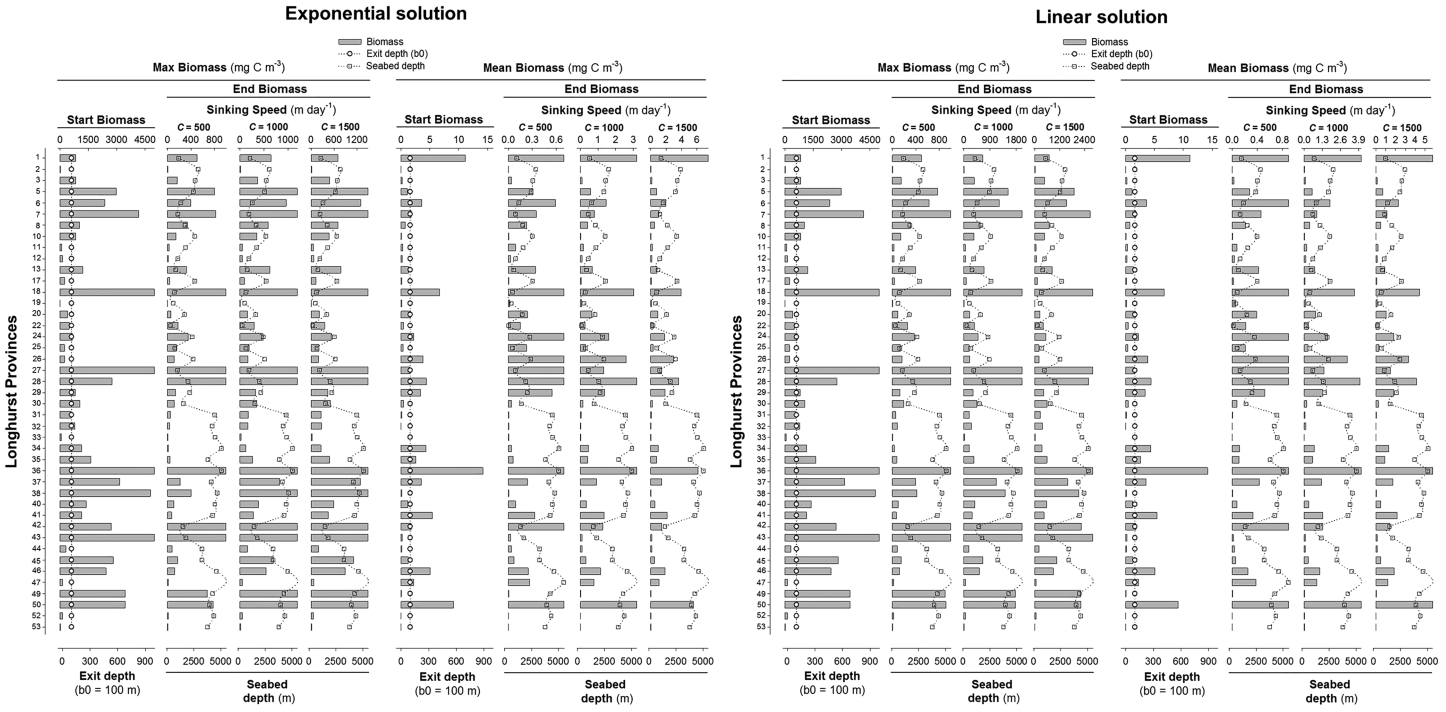

Figure 7. Solutions for exponential and linear temperature dependencies. The solutions are shown for start (100 m) and end (seabed) maximum and mean biomass for the 43 Longhurst Provinces using a matrix of three sinking speeds (C = 500, 1,000, and 1,500 m day^{-1}), and one exit depth (b0 = 100 m) representing the average of the euphotic zone. Biomass in several provinces exceeds the axis maximum, which values can be checked in Tables S1 (exponential) and S3 (linear).

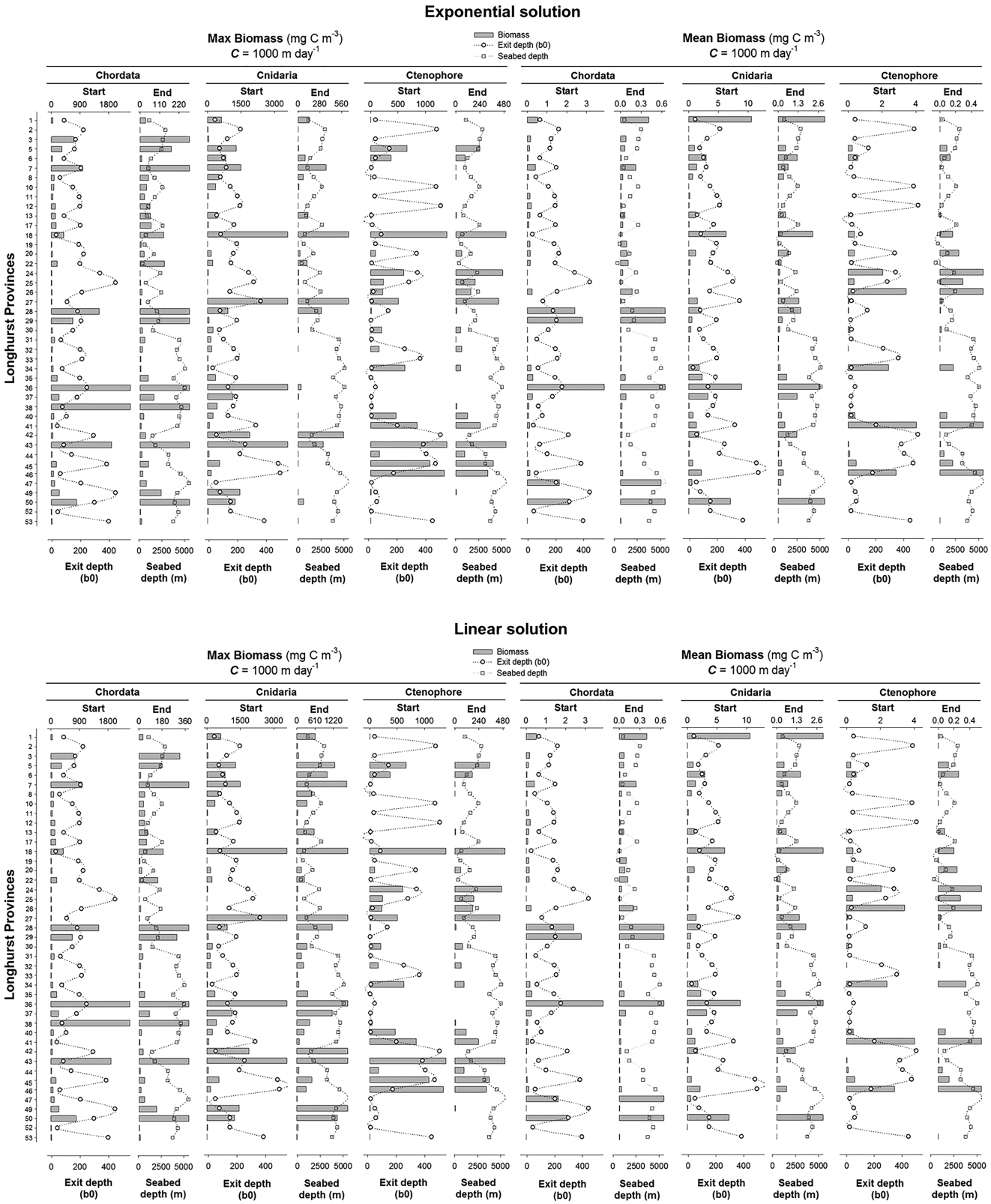

Figure 8. Solutions for exponential and linear temperature dependencies. The solutions are shown for start (phyla-province specific) and end (seabed) maximum and mean biomass for the 43 Longhurst Provinces using one sinking speed ($C = 1{,}000$ m day^{-1}) and specific exit depth (b0 = specific; see Figure 2 and Appendix C). Biomass in several provinces exceeds the axis maximum, which values can be checked in Tables S2 (exponential) and S4 (linear).

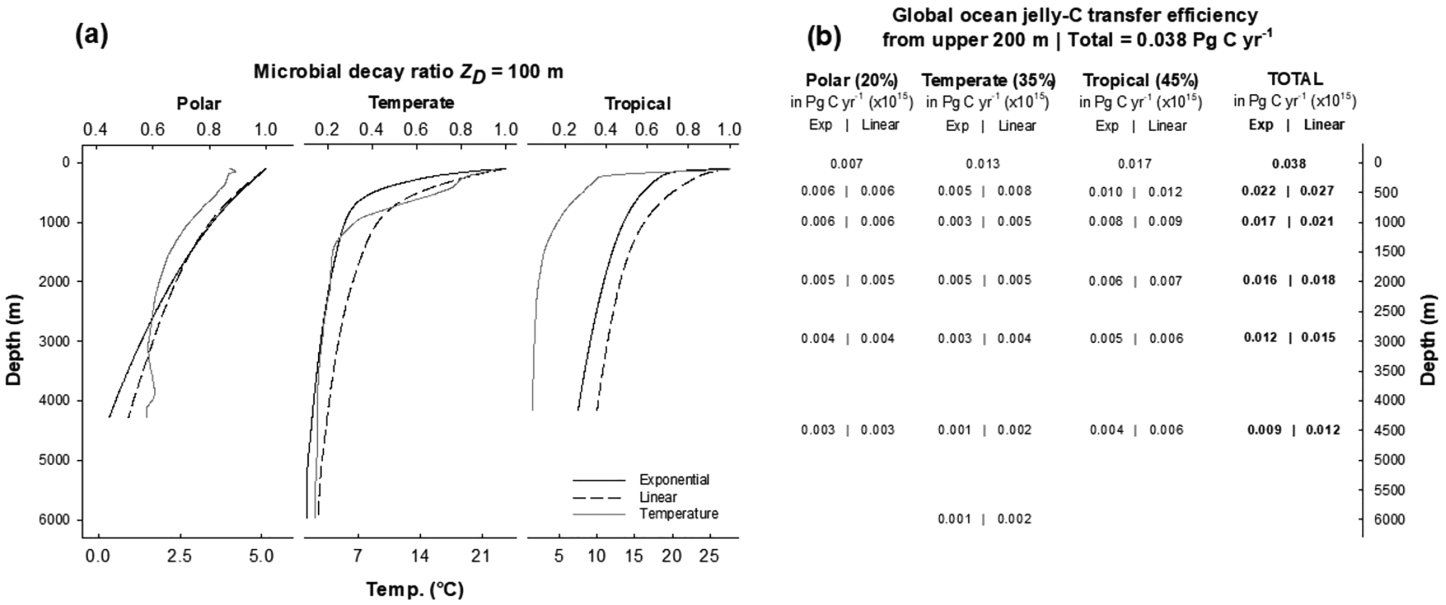

Figure 9. Solutions for exponential and linear temperature dependencies. (a) Averaged temperature profiles used to model global ocean jelly-C export from the upper 200 m (see section 2 for assumptions). (b) The numerical profiles show estimations (exponential and linear) of transferred jelly-C per latitude and depth (seabed) based on a total/initial production of 0.038 Pg C year^{-1} (1 Pg = 10^{15}) from the upper 200 m (Lucas et al., 2014), assuming turnover once a year (conservative since gelatinous zooplankton tend to live 2 to 6 months; see section 4).

1987). The jelly-C export contributes to pathway (i) by grazing, and to pathway (ii) as one of the major routes for particles reaching the deep ocean and the seabed.

Most knowledge about pathways (ii) and (iii) comes from sediment trap measurements at various depths that reflect particles originating in primary and secondary production, detritus, fecal material, or even material already processed by gelatinous zooplankton. For technical reasons, most sinking jelly-C (corpses, live bodies, decaying material) does not reach the traps and this flux is thus not quantified. Trap data are then extrapolated via parameterizations in global models (Honjo et al., 2008; Martin et al., 1987). About 5% to 25% of global net primary production (~50 Pg C year^{-1}; Field et al., 1998) is transferred from the euphotic zone to below 200 m (Buesseler, 1998; Schlitzer, 2000), and about 1% to 3% reaches the deep-sea below 3,000 m. Other estimates suggest that less than 15% of organic carbon leaving the euphotic zone reaches depths greater than 1,000 m because the remainder is remineralized or consumed at shallower depths (Buesseler et al., 2007; Buesseler & Boyd, 2009; Marsay et al., 2015). Open ocean sediment trap data (e.g., Buesseler et al., 2007) reveal total export ratios out of the euphotic zone between 0.20 and 0.50 at 500 m, indicating high remineralization rates, while the Martin curve predicts an export ratio of ~0.27 at 500 m. Detailed open ocean sediment trap investigations (summarized in Buesseler & Boyd, 2009) reach the same conclusion: between 80% and 90% of the carbon leaving the euphotic zone is remineralized above 1,000 m, and not more than 20% of the particulate carbon (POC) reaches 500 m. There is also a large contribution from fecal pellets, e.g., of copepod- and euphausiid-dominated zooplankton communities adding up in some cases to >90% of the total particulate organic carbon export (Belcher et al., 2017; Clarke et al., 1998).

Considering the different transfer efficiencies associated with pathways (ii), in particular the contribution of jelly-C, and (iii), the question arises: What are the major controls of transfer efficiency, and what are the implications, e.g., in zooplankton communities dominated by jelly-C, copepods, or euphausiids? Microbially mediated decay rates for copepod fecal pellets and marine snow range from 0.08 to 0.21 day^{-1} (Ploug et al., 2008; Ploug & Grossart, 2000), and for phytodetritus from 0.05 to 0.30 day^{-1} (Fujii et al., 2002; Sudo et al., 1978; Sweetman et al., 2014). While these decay rates are much lower than those associated with jelly-C (Figure 3), the phytodetritus and fecal particles and aggregates also remain much longer in the euphotic zone, owing to lower sinking velocities (from <1–100 m day^{-1} for phytodetritus, Mei et al., 2003, to between 100 and 500 m day^{-1} for fecal particles, reviewed by Turner, 2002). Hence, more time is available for remineralization and grazing, facilitating recycling (Huston & Deming, 2002), and preventing efficient

transfer to deeper water masses. The loss of carbon from the jelly-C via respiration and finite growth efficiency when acquiring carbon via grazing is considered only implicitly. For scyphozoans, at maximal growth rate, respiration reaches roughly 66% of assimilation, while production reaches 34%, with a net growth efficiency ranging from 35% to 37% (Fraser, 1969; Olesen et al., 1994). For salps, net growth efficiency is above 40% (Madin & Purcell, 1992; Zeldis et al., 1995). The associated carbon losses are all implicitly contained in our estimated flux profiles.

The factors controlling the transfer of phytodetritus, marine snow/aggregates, and small zooplankton fecal pellets from the euphotic zone to depth are interrelated processes, such as aggregation, disaggregation, microbial activity, scavenging, predation, detritus production, and mineral ballasting (De La Rocha & Passow, 2007). The transfer efficiency of jelly-C in pathway (ii) as Cnidaria, Ctenophora, and Thaliacea is estimated at 80% (Polar), 40% (Temperate), and 60% (Tropical) at 1,000 m and 50% (Polar), 20% (Temperate), and 30% (Tropical) at 4,000 m (Figure 9). In certain areas, jelly-C transfer efficiencies below 3,000 m are about one order of magnitude higher than estimates for other pathways, but the jelly-C fluxes remain transient in nature.

Our findings do not argue against the importance of phytoplankton- and smaller zooplankton-derived carbon, which is much larger than jelly-C, but demonstrate a higher transfer efficiency of the jelly-C export flux than some carbon vectors in certain areas, and situations, in particular around large gelatinous blooms and mass deposition events (e.g., Figure 6). Remineralization and downward-transfer of primary and secondary production by phytoplankton and small zooplankton behaves differently and should be considered separately from jelly-C, even though all ultimately originate from the same carbon source. While phytoplankton, fecal, and marine snow particles are heavily remineralized in the upper water column in relatively close proximity to the atmosphere, jelly-C is quickly transferred to the deep ocean (except in shallow shelf seas), contributing greatly to the deep-ocean pools of DOC and DIC.

A jelly-C dominated zooplankton community, which often occurs at the local and regional scale, not only increases the transfer efficiency via sinking (dead) jelly-C biomass, but also via active jelly-C fecal pellets production during bloom events (Bruland & Silver, 1981; Caron et al., 1989; Henschke et al., 2019; Iversen et al., 2016; Perissinotto & Pakhomov, 1998). Jelly-C fecal pellets are rich in carbon and nitrogen, are slowly degraded by microbes (Caron et al., 1989; Iversen et al., 2016), and sink fast, in some cases faster than 2,000 m day^{-1} (doliolids and salps; Turner, 2002). Jelly-C fecal pellets contribute greatly to the total organic carbon flux at various depth intervals (100 to 2,000 m), between 30% and 60% on average, depending on the location (Pakhomov et al., 2002; reviewed by Gleiber et al., 2012; Henschke et al., 2019; Turner, 2002). Although jelly-C fecal pellets and biomass transfer contribute significantly to the vertical flux of organic carbon, both pathways are highly intermittent, restricted to jelly bloom events and subsequent collapses. Including the pathways associated with jelly-C in local and regional models, and potentially in global carbon export models, should be considered a high priority.

4.2. Ecological Consequences of Fast Jelly-C Transfer

Jelly-C and other particulate carbon fluxes contribute greatly to the food demands of both pelagic and benthic organisms. Jelly-C in situ benthic measurements reveal in some cases C and N fluxes of 96% and 160% of the phytodetrital C and N, respectively, arriving at the seabed in the same area (Sweetman & Chapman, 2015). This exemplifies our estimates of maximal jelly-C biomass transfer efficiency for mass deposition events, transferring sudden large pulses of jelly-C to the seabed (Figure 6). During a mass-deposition event, starting from 400–500 mg C m^{-3}, considerable amounts of jelly-C biomass (>100 mg C m^{-3}) reach the seabed anywhere due to the relatively low decay rates at the low temperatures below the thermocline. In some temperate and in all polar regions, between 50% and 80% of the upper ocean jelly-C biomass reaches the seabed, thus transferring most of the carbon leaving the exit depth (Figure 6). Deep-sea long-term monitoring of jelly-C deposition supports some of our model estimates, e.g., Smith et al. (2014) report nearly 40 mg of salp-derived jelly-C m^{-2} d^{-1} arriving at 3,400 m in the northeastern Pacific during their 6-month study period. For 2 months, the salp jelly-C covered 90% of the seafloor, and benthic megafaunal organisms increased sevenfold in density after the peak of jelly-C deposition.

An increased jelly-C transfer efficiency has ecological consequences derived from the sinking of large carcass quantities, and the accumulation of the biomass at various depths. We could not find published numerical

estimates of jelly-C biomass being consumed by other organisms, which would slightly decrease the transfer efficiency. Pelagic consumption rates would need to be estimated prior to implementing in future models. Jelly-C is first consumed in the water column either as living organisms or upon dying and during sinking. The list of pelagic organisms known to consume jelly-C is growing (20% to 40% of the diet in some species, and up to 80% in others), especially after the increasing use of Stable Isotope Analyses, and includes tuna, billfish, mackerel and penguin species, sun fish, turtles, fish larvae, and juveniles, just to name a few (Cardona et al., 2012; Hays et al., 2018; Llopiz et al., 2010; Sampey et al., 2007; Thiebot et al., 2017). Jelly-C is also consumed by microbes during the initial sinking stages via preferential N-rich gelatinous biomass consumption, leaving behind carbon-enriched jelly-C (Tinta et al., 2016). The presence of jelly-C can also trigger changes in bacterial community structure (Titelman et al., 2006). The influence of sinking jelly-C on the microbial loop is likely rather ephemeral owing to the high sinking speed of jelly-C. On its way to the seafloor, jelly-C is often partly scavenged (Lebrato & Jones, 2009; Sweetman et al., 2014), but it can also arrive intact (Billett et al., 2006). The response of benthic macrofaunal/megafaunal communities to deposited jelly-C is largely unknown, except for baited experiments (Dunlop et al., 2017; Sweetman et al., 2014) and fixed stations at single depths (Smith et al., 2014). Part of the jelly-C is eventually consumed and remineralized by bacteria after arrival at the seabed (Sweetman et al., 2016; Titelman et al., 2006), leading to shifts in dissolved nutrients and carbon (Chelsky et al., 2015) and decreased oxygen levels (Pitt et al., 2009; West et al., 2009). Before microbes respire jelly-C at the seabed, much of it is often rapidly consumed by megafaunal organisms including fish, crustaceans, echinoderms, and arthropods (Lebrato & Jones, 2009; Smith et al., 2016; Sweetman et al., 2014). To what extent episodic jelly-C falls can affect macrofaunal and megafaunal communities remains unknown, but it is expected to exert a temporarily strong ecological effect in areas where jelly-C falls with a high transfer efficiency create sudden patches of food at the seabed (Ruhl, 2007).

4.3. Toward Including Jelly-C Transfer Efficiency in Biogeochemical Models

The jelly-C biomass transfer efficiency estimates rely on a model which depends strongly on the assumed gelatinous biomass decay rate (k), and its temperature dependence according to the exponential or linear solution (Figure 3). The exponential temperature dependency has a theoretical foundation in thermodynamics, but there is no theoretical support for the linear dependency. However, the exponential solution predicts very high decay rates at high temperatures, which suggest very fast biomass dissolution in the upper water column, similar to particle flux studies (Martin et al., 1987). This phenomenon may apply to certain jelly-C biomass types (ctenophores, hydrozoans, certain salps), but such results are not commonly observed in the field (Sweetman et al., 2016; Titelman et al., 2006). In fact, benthic surveys show that carcasses from different phyla/species can arrive almost intact in shape at the seabed (Billett et al., 2006; Lebrato & Jones, 2009; Smith et al., 2014). Therefore, until a larger data set on jelly-C biomass decay rates is produced from a range of robust laboratory or field decay experiments at various temperatures across several gelatinous zooplankton taxa, it remains unclear whether exponential or linear formulations should be used. High jelly-C decay rates at high temperatures imply increased microbially mediated decomposition during the initial sinking stages from 100 to 500 m, whereas decay rates slow down below due to lower temperatures. Jelly-C biomass from deeper water masses, e.g., from the mesopelagic zone, starts from a deeper b0, which translates into reduced decay rates with the potential to arrive in a more intact condition at the seabed.

Jelly-C biomass transfer efficiency is highly dependent on sinking rate. Owing to the large size of the carcasses, most sink faster than 800 m day^{-1}, and we assume a global mean of 1,000 m day^{-1} (Lebrato, Molinero, et al., 2013). Yet the sinking rate could also be affected by the remineralization itself and carcass fragmentation (affecting remineralization rate too; Frost et al., 2012), which will make sinking speed variable. Another factor not considered in this study is that jelly-C "particles" have a wide range of sizes, from milligrams to many kilograms, thus decay rates could be higher in smaller particles, which has not been considered owing to the absence of empirical data. To date, only the study of Titelman et al. (2006) on jellyfish has considered decay rate as a function of size, suggesting that the temperature effect is dominant over size, at least for very large particles such as jelly-C. For smaller particles, size and temperature both are critical during remineralization (Brown et al., 2004; Cavan et al., 2017). Yet this has only been tested at low temperatures. Experiments need to address decay rates including the size component in a temperature range comparable to the ocean at various latitudes to accurately target a wide variety of gelatinous zooplankton groups. These aspects cannot be accounted for in this study because there are no experimental studies

linking sinking rate, remineralization, fragmentation, and size. Fast sinking guarantees quick jelly-C transfer from 1,000 m down to 4,000–5,000 m. Transfer profiles differ among Longhurst Provinces, as they are based on the corresponding temperature profiles. The most efficient transfer from the euphotic zone occurs in polar regions (Figure 4) due to low temperatures in the whole water column, preventing major decay. When b0 is below the euphotic zone and the relatively warm thermocline, e.g., 500 or 1,000 m, the jelly-C transfer efficiency is similar across all latitudes. This is because the strong thermoclines in the upper ocean at temperate and tropical Longhurst provinces govern the jelly-C remineralization profiles (Figures 2 and 4). When grouping organisms by taxa and species, jelly-C export per Longhurst Province has a taxon- or species-specific component, which is presently difficult to determine. We acknowledge a variable jelly-C sinking speed and a variable b0 in the upper 500 m (Figure 5) depending on life history, which we have tried to account for as much as possible using wide ranges for sinking rate and b0. Deep jelly-C export originating at greater depths is difficult to assess because no reliable biomass and b0 data exist below 200–500 m, which could be used to estimate deep carbon export and transfer efficiency. This is somewhat unfortunate because large gelatinous zooplankton populations do live deeper than 500 m in the mesopelagic and bathypelagic zones (Robinson et al., 2010).

Other aspects to consider are that if a jelly-C sinking event is from a population living below 500 m, the carbon flux derives from already exported carbon from the upper ocean (potentially reprocessed already by other gelatinous zooplankton), since export flux is commonly defined at carbon being exported below 150 m. Since all jelly-C ultimately derives from primary production, the actual effect of fast sinking jelly-C is an acceleration of the transfer between the upper 500 m and the deep ocean, thus an increased transfer efficiency. The amounts of jelly-C and microbial decay rates defined here as well as the high sinking speeds guarantee an accelerated carbon transfer to the deep ocean. It also needs to be considered that scyphozoans net growth efficiency is above 30% (Fraser, 1969; Olesen et al., 1994), and that for salps, it is above 40% (Madin & Purcell, 1992; Zeldis et al., 1995), which constitutes a loss of fixed carbon from upper levels, that is then not exported to depth. Corrected for the Longhurst Province area, 59–72% of the jelly-C leaving the upper 200 m arrives at 500 m, 46–54% at 1,000 m, 43–48% at 2,000 m, 32–40% at 3,000 m, and 25–33% at 4,500 m. The ~0.038 Pg C $year^{-1}$ upper ocean gelatinous zooplankton production translates into about 0.02–0.03, 0.02, and 0.01 Pg C $year^{-1}$ being transferred down to 500, 2,000, and 4,500 m, respectively (Figure 9). The jelly-C biomass production rate of 0.038 Pg C $year^{-1}$ can be considered conservative considering that the JeDI database covers less than 50% of the global ocean. This previously ignored carbon export flux is significant compared to total ocean carbon export as estimated from sediment-trap data, permanently transferred to the ocean interior, i.e., below the permanent thermocline, and thus forms an important component of the global biological soft-tissue pump to be urgently considered in local, regional, and potentially global biogeochemical models.

Appendix A

Raw collection depth data used to work out exit depths (b0) (Figure 2). Original data belong to the Jellyfish Database Initiative (JeDI: https://jedi.nceas.ucsb.edu), including public data sets (https://www.bco-dmo.org/dataset/526852)

Appendix B

Raw metadata and phylum data used in all calculations. Original biomass data belong to Lucas et al. (2014) and are used under John Wiley and Sons License Number 4160191181614. The rest was newly compiled from the Jellyfish Database Initiative (JeDI: https://jedi.nceas.ucsb.edu), including public data sets (http://www.bco-dmo.org/dataset/526852).

Appendix C

GLODAPv2 spreadsheet with the original depth and temperature profiles used to work out export ratios for individual Longhurst Provinces.

Appendix D

Excel spreadsheet to work out microbial decay ratios and biomass using any kind of initial conditions using the exponential and linear solutions (Table 1). There is also a comparison between polar, temperate, and tropical latitudes to show how the exponential and linear solutions change depending on the input temperature profiles.

Appendix E

Exponential and linear equation full solutions on the model parameterizations.

Acknowledgments
This study was developed under a grant from the Federal Ministry of Education and Research (BMBF) to ML and JCM under contract No. 03F0722A. The original work started with funding by the Kiel Cluster of Excellence "The Future Ocean" (D1067/87) to AO and ML, and also by the "European Project on Ocean Acidification" (which received funding from the European Community's Seventh Framework Programme [FP7/2007–2013] under grant agreement 211384) to AO and ML. Readers can access data in a raw format in the BCO-DMO data management office (https://www.bco-dmo.org/dataset/526852), and in the format used in this publication at the NOAA National Center for Environmental Information (NCEI) under Accession Number 0207402 in https://data.nodc.noaa.gov/cgi-bin/iso?id=gov.noaa.nodc:0207402.

References

Andersen, K. H., Berge, T., Goncalves, R. J., Hartvig, M., Heuschele, J., Hylander, S., et al. (2016). Characteristic sizes of life in the oceans, from Bacteria to Whales. *Annual Review of Marine Science*, *8*(1), 217–241. https://doi.org/10.1146/annurev-marine-122414-034144

Asper, V. L. (1987). Measuring the flux and sinking speed of marine snow aggregates. *Deep Sea Research*, *34*(1), 1–17. https://doi.org/10.1016/0198-0149(87)90117-8

Ates, R. M. L. (2017). Benthic scavengers and predators of jellyfish, material for a review. *Plankton and Benthos Research*, *12*(1), 71–77. https://doi.org/10.3800/pbr.12.71

Beaulieu, S. (2002). Accumulation and fate of phytodetritus on the seafloor. *Oceanography and Marine Biology*, *40*, 171–232.

Behrenfeld, M. J., & Falkowski, P. G. (1997). Photosynthetic rates derived from satellite-based chlorophyll concentration. *Limnology and Oceanography*, *42*(1), 1–20. https://doi.org/10.4319/lo.1997.42.1.0001

Belcher, A., Manno, C., Ward, P., Henson, S. A., Sanders, R., & Tarling, G. A. (2017). Copepod faecal pellet transfer through the meso- and bathypelagic layers in the Southern Ocean in spring. *Biogeosciences*, *14*(6), 1511–1525. https://doi.org/10.5194/bg-14-1511-2017

Billett, D. S. M., Bett, B. J., Jacobs, C. L., Rouse, I. P., & Wigham, B. D. (2006). Mass deposition of jellyfish in the deep Arabian Sea. *Limnology and Oceanography*, *51*(5), 2077–2083. https://doi.org/10.4319/lo.2006.51.5.2077

Brotz, L., William, W. L., Cheung, K. K., Pakhomov, E., & Pauly, D. (2012). Increasing jellyfish populations: Trends in large marine ecosystems. *Hydrobiologia*, *690*(1), 3–20. https://doi.org/10.1007/s10750-012-1039-7

Brown, J. H., Gillooly, J. F., Allen, A. P., Savage, V. M., & West, G. B. (2004). Toward a metabolic theory of ecology. *Ecology*, *85*(7), 1771–1789. https://doi.org/10.1890/03-9000

Bruland, K. W., & Silver, M. W. (1981). Sinking rates of fecal pellets from gelatinous zooplankton (Salps, Pteropods, Doliolids). *Marine Biology Heidelberg*, *63*(3), 295–300. https://doi.org/10.1007/BF00395999

Buesseler, K. O. (1998). The decoupling of production and particulate export in the surface ocean. *Global Biogeochemical Cycles*, *12*(2), 297–310. https://doi.org/10.1029/97GB03366

Buesseler, K. O., & Boyd, P. W. (2009). Shedding light on processes that control particle export and flux attenuation in the twilight zone of the open ocean. *Limnology and Oceanography*, *54*(4), 1210–1232. https://doi.org/10.4319/lo.2009.54.4.1210

Buesseler, K. O., Lamborg, C. H., Boyd, P. W., Lam, P. J., Trull, T. W., Bidigare, R. R., et al. (2007). Revisiting carbon flux through the ocean's twilight zone. *Science*, *316*(5824), 567–570. https://doi.org/10.1126/science.1137959

Cacchione, D. A., Rowe, G. T., & Malahoff, A. (1978). Submersibleinvestigation of outer Hudson submarine canyon. In D. J. Stanley, G. Kelling (Eds.), *Sedimentation in submarinecanyons, fans and trenches. Dowden Hutchinson & Ross, Stroudsburg, PA* (pp. 42–50. (21) (PDF) Salp-falls in the Tasman Sea: A major food input to deepsea benthos. Retrieved from https://www.researchgate.net/publication/273269364_Salp-falls_in_the_Tasman_Sea_A_major_food_input_to_deep-sea_benthos [accessed Dec 22 2019]

Cardona, L., de Quevedo, I. A., Borrel, A., & Aguilar, A. (2012). Massive consumption of gelatinous plankton by Mediterranean apex predators. *PLoS ONE*, *7*(3), e31329. https://doi.org/10.1371/journal.pone.0031329

Caron, D. A., Madin, L. P., & Cole, J. J. (1989). Composition and degradation of salp fecal pellets: Implications for vertical flux in oceanic environments. *Journal of Marine Research*, *47*(4), 829–850. https://doi.org/10.1357/002224089785076118

Cavan, E. L., Trimmer, M., Shelley, F., & Sanders, R. (2017). Remineralization of particulate organic carbon in an ocean oxygen minimum zone. *Nature Communications*, *8*, 14847. https://doi.org/10.1038/ncomms14847

Ceh, J., Gonzalez, J., Pacheco, A., & Riascos, J. M. (2015). The elusive life cycle of scyphozoan jellyfish—Metagenesis revisited. *Scientific Reports*, *5*, 12037. https://doi.org/10.1038/srep12037

Chelsky, A., Pitt, K. A., & Welsh, D. T. (2015). Biogeochemical implications of decomposing jellyfish blooms in a changing climate. *Estuarine, Coastal and Shelf Science*, *154*, 77–83. https://doi.org/10.1016/j.ecss.2014.12.022

Clarke, A., Quetin, L. B., & Ross, R. M. (1998). Laboratory and field estimates of the rate of faecal pellet production by Antarctic krill, *Euphausia superb*. *Marine Biology*, *98*, 557–563.

Condon, R. H., Duarte, C. M., Pitt, K. A., Robinson, K. L., Lucas, C. H., Sutherland, K. R., et al. (2013). Recurrent jellyfish blooms are a consequence of global oscillations. *Proceedings of the National Academy of Sciences*, *110*(3), 1000–1005. https://doi.org/10.1073/pnas.1210920110

Condon, R. H., Graham, W. M., Duarte, C. M., Pitt, K. A., Lucas, C. H., Haddock, S. H. D., et al. (2012). Questioning the rise of gelatinous zooplankton in the world's oceans. *Bioscience*, *62*, 161–169.

Condon, R.H., C. Lucas, C. M. Duarte, and K. A. Pitts (eds.) (2015), JeDI: The jellyfish database initiative Santa Barbara, US. National Center for Ecological Analysis and Synthesis (NCEAS)

Condon, R. H., Steinberg, D. K., del Giorgio, P. A., Bouvier, T. C., Bronk, D. A., Graham, W., & Ducklow, H. W. (2011). Jellyfish blooms result in a major microbial respiratory sink of carbon in marine systems. *Proceedings of the National Academy of Sciences*, *108*(25), 10,225–10,230. https://doi.org/10.1073/pnas.1015782108

De La Rocha, C., & Passow, U. (2007). Factors influencing the sinking of POC and the efficiency of the biological carbon pump. *Deep SeaRes. Part II* (54(5), pp. 639–658).

Dunlop, K. M., Jones, D. O. B., & Sweetman, A. K. (2017). Direct evidence of an efficient energy transfer pathway from jellyfish carcasses to a commercially important deep-water species. *Scientific Reports*, *7*, 17455. https://doi.org/10.1038/s41598-017-17557-x

Field, C., Behrenfeld, M., Randerson, J., & Falkowski, P. (1998). Primary production in the biosphere: Integrating terrestrial and oceanic components. *Science*, *281*, 237–241. https://doi.org/10.1126/science.281.5374.237

Fraser, J. H. (1969). Experimental feeding of some medusae and chaetognatha. *Journal of the Fisheries Research Board of Canada*, *26*(7), 1743–1762. https://doi.org/10.1139/f69-161

Frost, J. R., Jacoby, C. A., Frazer, T. K., & Zimmerman, A. R. (2012). Pulse perturbations from bacterial decomposition of *Chrysaora quinquecirrha* (Scyphozoa: Pelagiidae). *Hydrobiologia*, *690*(1), 247–256. https://doi.org/10.1007/s10750-012-1042-z

Fujii, M., Murashige, S., Ohnishi, Y., Yuzawa, A., Miyasaka, H., Suzuki, Y., & Komiyama, H. (2002). Decomposition of phytoplankton in seawater. Part I: Kinetic analysis of the effect of organic matter concentration. *Journal of Oceanography*, *58*(3), 438–443. https://doi.org/10.1023/A:1021296713132

Gehlen, M., Bopp, L., Emprin, N., Aumont, O., Heinze, C., & Ragueneau, O. (2006). Reconciling surface ocean productivity, export fluxes and sediment composition in a global biogeochemical ocean model. *Biogeosciences*, *3*(4), 521–537. https://doi.org/10.5194/bg-3-521-2006

Gleiber, M. R., Steinberg, D. K., & Ducklow, H. W. (2012). Time series of vertical flux of zooplankton fecal pellets on the continental shelf of the western Antarctic Peninsula. *Marine Ecology Progress Series*, *471*, 23–36. https://doi.org/10.3354/meps10021

Hays, G. C., Doyle, T. K., & Houghton, D. R. (2018). A paradigm shift in the trophic importance of jellyfish. *Trends in Ecology & Evolution*, *33*(11), 874–884. https://doi.org/10.1016/j.tree.2018.09

Henschke, N., Pakhomov, E. A., Kwong, L. E., Everett, J. D., Laiolo, L., Coghlan, A. R., & Suthers, I. M. (2019). Large vertical migrations of *Pyrosoma atlanticum* play an important role in active carbon transport. *Journal of Geophysical Research: Biogeosciences*, *124*(5), 1056–1070. https://doi.org/10.1029/2018JG004918

Honjo, S., Manganini, S. J., KrishField, R. A., & Francois, R. (2008). Particulate organic carbon fluxes to the ocean interior and factors controlling the biological pump: A synthesis of global sediment trap programs since 1983. *Progress in Oceanography*, *76*(3), 217–285. https://doi.org/10.1016/j.pocean.2007.11.003

Huston, A. L., & Deming, J. W. (2002). Relationships between microbial extracellular enzymatic activity and suspended and sinking particulate organic matter: Seasonal transformations in the North Water. *Deep Sea Research*, *49*(22-23), 5211–5225. https://doi.org/10.1016/S0967-0645(02)00186-8

Iguchi, N., R. Ishikawa, O. Sato, T. Onishi, and T. Maeda (2006), Decomposition rate of the giant jellyfish *Nemopilema nomurai* in Sado Island. [Translated from Japanese.] FRA, Japan Sea National Fisheries Research Institute report [accessed 2009 June 2]. Available from http://jsnfri.fra.affrc.go.jp/Kurage/kurage_hp18/Sado_bunkai.pdf

Ilyina, T., Six, K. D., Segschneider, J., Maier-Reimer, E., Li, H., & Nunez-Riboni, I. (2013). The global ocean biogeochemistry model HAMOCC: Model architecture and performance as component of the MPI-Earth System Model in different CMIP5 experimental realizations. *Journal of Advances in Modeling Earth Systems*, *5*, 287–315. https://doi.org/10.1029/2012MS000178

Iversen, M. H., Pakhomov, E. A., Hunt, B. P. V., van der Jagt, Wolf-Gladrow, D., & Klaas, C. (2016). Sinkers or floaters? Contribution from salp pellets to the export flux during a large bloom event in the Southern Ocean. *Deep Sea Research*, *138*, 116–125. https://doi.org/10.1016/j.dsr2.2016.12.004

Jackson, G. A., Maffione, R., Costello, D. K., Alldredge, A. L., Logan, B. E., & Dam, H. G. (1997). Particle size spectra between 1 mm and 1 cm at Monterey Bay determined using multiple instruments. *Deep Sea Research*, *45*, 1739–1767.

Key, R. M., A. Olsen, S. van Heuven, S. K. Lauvset, A. Velo, X. Lin, et al. (2015), Global Ocean Data Analysis Project, version 2. ORNL/CDIAC-162 NDP-093

Koppelmann, R., & Frost, J. (2008). The ecological role of zooplankton in the twilight and dark zones of the ocean. In L. P. Mertens (Ed.), *Biological Oceanography Research Trends*, (pp. 67–130). New York: Nova Science Publishers, Inc.

Laufkötter, C., Vogt, M., Gruber, N., Aita-Noguchi, M., Aumont, O., Bopp, L., et al. (2015). Drivers and uncertainties of future global marine primary production in marine ecosystem models. *Biogeosciences*, *12*(23), 6955–6984. https://doi.org/10.5194/bg-12-6955-2015

Lebrato, M., de Jesus Mendes, P., Steinberg, D. K., Cartes, J. E., Jones, B. M., Birsa, L. M., et al. (2013). Jelly biomass sinking speed reveals a fast carbon export mechanism. *Limnology and Oceanography*, *58*(3), 1113–1122. https://doi.org/10.4319/lo.2013.58.3.1113

Lebrato, M., & Jones, D. O. B. (2009). Mass deposition event of *Pyrosoma atlanticum* carcasses off Ivory Coast (West Africa). *Limnology and Oceanography*, *54*(4), 1197–1209. https://doi.org/10.4319/lo.2009.54.4.1197

Lebrato, M., Molinero, J.-C., Cartes, J. E., Lloris, D., Melin, F., & Beni-Casadella, L. (2013). Sinking jelly-C unveils potential environmental variability along a continental margin. *PLoS ONE*, *8*, e82070. https://doi.org/10.1371/journal.pone.0082070

Lebrato, M., Pahlow, M., Oschlies, A., Pitt, K. A., Jones, D. O. B., Molinero, J.-C., & Condon, R. H. (2011). Depth attenuation of organic matter export associated with jelly falls. *Limnology and Oceanography*, *56*(5), 1917–1928. https://doi.org/10.4319/lo.2011.56.5.1917

Lebrato, M., Pitt, K. A., Sweetman, A. K., Jones, D. O. B., Cartes, J. E., Oschlies, A., et al. (2012). Jelly-falls historic and recent observations: A synthesis to drive future research directions. *Hydrobiologia*, *690*(1), 227–245. https://doi.org/10.1007/s10750-012-1046-8

Legendre, L. (1990). The significance of microalgal blooms for fisheries and for the export of particulate organic carbon in oceans. *Journal of Plankton Research*, *12*(4), 681–699. https://doi.org/10.1093/plankt/12.4.681

Llopiz, J. K., Richardson, D. E., Shiroza, A., Smith, S. L., & Cowen, R. K. (2010). Distinctions in the diets and distributions of larval tunas and the important role of appendicularians. *Limnology and Oceanography*, *55*(3), 983–996. https://doi.org/10.4319/lo.2010.55.3.0983

Lombard, F., & Kiørboe, T. (2010). Marine snow originating from appendicularian houses: Age-dependent settling characteristics. *Deep Sea Research*, *57*(10), 1304–1313. https://doi.org/10.1016/j.dsr.2010.06.008

Lombard, F., Legendre, L., Picheral, M., Sciandra, A., & Gorsky, G. (2010). Prediction of ecological niches and carbon export by appendicularians using a new multispecies ecophysiological model. *Marine Ecology Progress Series*, *398*, 109–125. https://doi.org/10.3354/meps08273

Longhurst, A. R. (1995). Seasonal cycles of pelagic production and consumption. *Progress in Oceanography*, *36*(2), 77–167. https://doi.org/10.1016/0079-6611(95)00015-1

Longhurst, A. R. (1998). *Ecological geography of the sea*, (p. 398). San Diego: Academic Press.

Lucas, C. H., Jones, D. O. B., Hollyhead, C. J., Condon, R. H., Duarte, C. M., Graham, W. M., et al. (2014). Gelatinous zooplankton biomass in the global oceans: Geographic variation and environmental drivers. *Global Ecology and Biogeography*, *23*(7), 701–714. https://doi.org/10.1111/geb.12169

Lucas, C. H., Pitt, K. A., Purcell, J. E., Lebrato, M., & Condon, R. H. (2011). What's in a jellyfish? Proximate and elemental composition and biometric relationships for use in biogeochemical studies. *Ecology*, *92*, 1704. https://doi.org/10.1890/11-0302.1

Madin, L. P., & Purcell, J. E. (1992). Feeding, metabolism, and growth of *Cyclosalpa bakeri* in the subarctic Pacific. *Limnology and Oceanography*, *37*(6), 1236–1251. https://doi.org/10.4319/lo.1992.37.6.1236

Marsay, C. M., Sanders, R. J., Henson, S. A., Pabortsava, K., Achterberg, E. P., & Lampitt, R. (2015). Attenuation of sinking particulate organic carbon flux through the mesopelagic ocean. *Proceedings of the National Academy of Sciences of the United States of America*, *112*(4), 1089–1094. https://doi.org/10.1073/pnas.1415311112

Martin, J. H., Knauer, G. A., Karl, D. M., & Broenkow, W. W. (1987). VERTEX: Carbon cycling in the northeast Pacific. *Deep Sea Research, Part I*, *34*(2), 267–285. https://doi.org/10.1016/0198-0149(87)90086-0

McDonnell, A. M. P., & Buesseler, K. O. (2010). Variability in the average sinking velocity of marine particles. *Limnology and Oceanography*, *55*(5), 2085–2096. https://doi.org/10.4319/lo.2010.55.5.2085

Mei, Z. P., Legendre, L., Gratton, Y., Tremblay, J. E., LeBlanc, B., Klein, B., & Gosselin, M. (2003). Phytoplankton production in the North Water Polynya: size-fractions and carbon fluxes, April–July 1998. *Marine Ecology Progress Series*, *256*, 13–27. https://doi.org/10.3354/meps256013

Moore, J. K., Doney, S. C., & Lindsay, K. (2004). Upper ocean ecosystem dynamics and iron cycling in a global three-dimensional model. *Global Biogeochemical Cycles*, *18*, GB4028. https://doi.org/10.1029/2004GB002220

Moriarty, R., & O'Brien, T. D. (2013). Distribution of mesozooplankton biomass in the global ocean. *Earth System Science Data*, *5*(1), 45–55. https://doi.org/10.5194/essd-5-45-2013

Olesen, N. J., Frandsen, K., & Riisgard, H. U. (1994). Population dynamics, growth and energetics of jellyfish Aurelia aurita in a shallow fjord. *Marine Ecology Progress Series*, *105*, 9–18. https://doi.org/10.3354/meps105009

Pakhomov, E., Froneman, P. W., & Perissinotto, R. (2002). Salp/krill interactions in the Southern Ocean: Spatial segregation and implications for the carbon flux. *Deep Sea Research*, *49*(9-10), 1881–1907. https://doi.org/10.1016/S0967-0645(02)00017-6

Pauly, D., Graham, W. M., Libralato, S., Morissette, L., & Palomares, M. L. D. (2009). Jellyfish in ecosystems, online databases, and ecosystem models. *Hydrobiologia*, *616*(1), 67–85. https://doi.org/10.1007/s10750-008-9583-x

Peinert, R., von Bodungen, B., & Smetacek, V. S. (1989). Food web structure and loss rate. In W. H. Berger, V. S. Smetacek, & G. Wefer (Eds.), *Productivity of the ocean: present and past*, (pp. 35–48). New York: John Wiley & Sons.

Perissinotto, R., & Pakhomov, E. A. (1998). Contribution of salps to carbon flux of marginal ice zone of the Lazarev Sea, Southern Ocean. *Marine Biodiversity*, *131*(1), 25–32. https://doi.org/10.1007/s002270050292

Pilskaln, C. H., & Honjo, S. (1987). The fecal pellets fraction of biogeochemical particle fluxes to the deep sea. *Global Biogeochemical Cycles*, *1*(1), 31–48. https://doi.org/10.1029/GB001i001p00031

Pitt, K. A., Welsh, D. T., & Condon, R. H. (2009). Influence of jellyfish blooms on carbon, nitrogen and phosphorus cycling and plankton production. *Hydrobiologia*, *616*(1), 133–149. https://doi.org/10.1007/s10750-008-9584-9

Ploug, H., & Grossart, H.-P. (2000). Bacterial growth and grazing on diatom aggregates: Respiratory carbon turnover as a function of aggregate size and sinking velocity. *Limnology and Oceanography*, *45*(7), 1467–1475. https://doi.org/10.4319/lo.2000.45.7.1467

Ploug, H., Iversen, M. H., & Fischer, G. (2008). Ballast, sinking velocity and apparent diffusivity within marine snow and fecal pellets: Implications and substrate turnover by attached bacteria. *Limnology and Oceanography*, *53*(5), 1878–1886. https://doi.org/10.4319/lo.2008.53.5.1878

Raskoff, K. A., Sommer, F. A., Hamner, W. M., & Cross, K. M. (2003). Collection and culture techniques for gelatinous zooplankton. *Biological Bulletin (Woods Hole)*, *204*(1), 68–80. https://doi.org/10.2307/1543497

Robinson, C., Steinberg, D. K., Anderson, T. R., Aristegui, J., Carlson, C. A., Frost, J. R., et al. (2010). Mesopelagic zone ecology and biogeochemistry—A synthesis. *Deep Sea Research*, *57*(16), 1504–1518. https://doi.org/10.1016/j.dsr2.2010.02.018

Robison, B. H., Reisenbichler, K. R., & Sherlock, R. E. (2005). Giant larvacean houses: Rapid carbon transport to the deep-sea floor. *Science*, *308*(5728), 1609–1611. https://doi.org/10.1126/science.1109104

Ruhl, H. A. (2007). Abundance and size distribution dynamics of abyssal epibenthic megafauna in the northeast Pacific. *Ecology*, *88*(5), 1250–1262. https://doi.org/10.1890/06-0890

Sampey, A., McKinnon, A. D., Meekan, M. G., & McCormick, M. I. (2007). Glimpse into guts: Overview of the feeding of larvae of tropical shorefishes. *Marine Ecology Progress Series*, *339*, 243–257. https://doi.org/10.3354/meps339243

Schlitzer, R. (2000). Applying the adjoint method for biogeochemical modeling: Export of particulate organic matter in the world ocean. In P. Kasibhata (Ed.), *Inverse Methods in Global biogeochemical Cycles*, *AGU Monograph*, (Vol. 114, pp. 107–124). Washington, DC: American Geophysical Union.

Sempere, R., Yoro, S. C., van Wambeke, F., & Charriere, B. (2000). Microbial decomposition of large organic particles in the northwestern Mediterranean Sea: An experimental approach. *Marine Ecology Progress Series*, *198*, 61–72. https://doi.org/10.3354/meps198061

Sieburth, J. M., Smetacek, V., & Lenz, J. (1978). Pelagic ecosystem structure: Heterotrophic compartments of the plankton and their relationship to plankton size fractions. *Limnology and Oceanography*, *23*(6), 1256–1263. https://doi.org/10.4319/lo.1978.23.6.1256

Siegel, D. A., Buesseler, K. O., Doney, S. C., Sailley, S. F., Behrenfeld, M. J., & Boyd, P. W. (2014). Global assessment of ocean carbon export by combining satellite observations and food-web models. *Global Biogeochemical Cycles*, *28*, 181–196. https://doi.org/10.1002/2013GB004743

Smith, B. E., Ford, M. D., & Link, J. S. (2016). Bloom or bust: Synchrony in jellyfish abundance, fish consumption, benthic scavenger abundance, and environmental drivers across a continental shelf. *Fisheries Oceanography*, *25*(5), 500–514. https://doi.org/10.1111/fog.12168

Smith, K. L. Jr., Sherman, A. D., Huffard, C. L., McGill, P. R., Henthorn, R., Von Thun, S., et al. (2014). Large salp bloom export from the upper ocean and benthic community response in the abyssal northeast Pacific: Day to week resolution. *Limnology and Oceanography*, *59*(3), 745–757. https://doi.org/10.4319/lo.2014.59.3.0745

Sudo, R., Ohtake, H., & Aiba, S. (1978). Some ecological observation on the decomposition of periphytic algae and aquatic plants. *Water Research*, *12*(3), 179–184. https://doi.org/10.1016/0043-1354(78)90006-4

Sweetman, A. K., & Chapman, A. (2011). First observations of moribund jellyfish at the seafloor in a deep-sea fjord. *Deep Sea Research*, *58*(12), 1206–1211. https://doi.org/10.1016/j.dsr.2011.08.006

Sweetman, A. K., & Chapman, A. C. (2015). First assessment of flux rates of jellyfish carcasses (jelly-falls) to the benthos reveals the importance of gelatinous material for biological C-cycling in jellyfish-dominated ecosystems. *Frontiers in Marine Science*, *2*, 47. https://doi.org/10.3389/fmars.2015.00047

Sweetman, A. K., Chelsky, A., Pitt, K. A., Andrade, H., van Oevelen, D., & Renaud, P. E. (2016). Jellyfish decomposition at the seafloor rapidly alters biogeochemical cycling and carbon flow through benthic food-webs. *Limnology and Oceanography*, *61*(4), 1449–1461. https://doi.org/10.1002/lno.10310

Sweetman, A. K., Smith, C. R., Dale, T., & Jones, D. O. B. (2014). Rapid scavenging of jellyfish carcasses reveals the importance of gelatinous material to deep-sea food webs. *Proceedings of the Royal Society B*, *281*, 20142210. https://doi.org/10.1098/rspb.2014.2210

Thiebot, J.-B., Arnould, J. P. Y., Gomez-Laich, A., Ito, K., Kato, A., Mattern, T., et al. (2017). Jellyfish and other gelata as food for four penguin species—Insights from predator-borne videos. *Frontiers in Ecology and the Environment*, *15*(8), 437–441. https://doi.org/10.1002/fee.1529

Tinta, T., Kogovsek, T., Turk, V., Shiganova, T. A., Mikaelyan, A. S., & Malej, A. (2016). Microbial transformation of jellyfish organic matter affects the nitrogen cycle in the marine water column—A Black Sea case study. *Journal of Experimental Marine Biology and Ecology*, *475*, 19–30. https://doi.org/10.1016/j.jembe.2015.10.018

Titelman, J., Riemann, L., Sørnes, T. A., Nilsen, T., Griekspoor, P., & Bamstedt, U. (2006). Turnover of dead jellyfish: Stimulation and retardation of microbial activity. *Marine Ecology Progress Series*, *325*, 43–58. https://doi.org/10.3354/meps325043

Turner, J. T. (2002). Zooplankton fecal pellets, marine snow and sinking phytoplankton blooms. *Aquatic Microbial Ecology*, *27*, 57–102. https://doi.org/10.3354/ame027057

Walsby, A. E., & Xypolyta, A. (1977). The form resistance of chitan fibres attached to the cells of *Thalassiosira fluviatilis* Hustedt. *British Journal of Psychology*, *12*(3), 215–223. https://doi.org/10.1080/00071617700650231

West, E. J., Welsh, D. T., & Pitt, K. A. (2009). Influence of decomposing jellyfish on sediment oxygen demand and nutrient dynamics. *Hydrobiologia*, *616*(1), 151–160. https://doi.org/10.1007/s10750-008-9586-7

Yamamoto, J., Hirose, M., Ohtani, T., Sugimoto, K., Hirase, K., Shimamoto, N., et al. (2008). Transportation of organic matter to the sea floor by carrion falls of the giant jellyfish *Nemopilema nomurai* in the Sea of Japan. *Marine Biology*, *153*(3), 311–317. https://doi.org/10.1007/s00227-007-0807-9

Zeldis, J. R., Davis, C. S., James, M. R., Ballara, S. L., Booth, W. E., & Chang, F. H. (1995). Salp grazing: Effects on phytoplankton abundance, vertical distribution and taxonomic composition in a coastal habitat. *Marine Ecology Progress Series*, *126*, 267–283. https://doi.org/10.3354/meps126267